THE UNIVERSITY of ADELAIDE
INSTITUTE FOR PHOTONICS & ADVANCED SENSING

GRAPE AND WINE RESEARCH AND DEVELOPMENT CORPORATION

SMART BUNGS



FINAL REPORT to

GRAPE AND WINE RESEARCH & DEVELOPMENT CORPORATION

Project Number: UA 1003

Principal Investigator: Professor Dennis K. Taylor

Research Organisation: The University of Adelaide University

Date: 1 November 2011

GRAPE AND WINE RESEARCH & DEVELOPMENT CORPORATION

Project Number: UA 1003

Title: SMART BUNGS

Authors: Professor Dennis K. Taylor
Professor Tanya Monro
Miss Mai-Chi Nguyen
Miss Rachel Moore

The University of Adelaide
School of Agriculture, Food and Wine
Private Mailbox 1
Glen Osmond, SA 5064, Australia
Telephone: (08) 83037239
Email: dennis.taylor@adelaide.edu.au

Acknowledgements: Research and activities in the project covered by this report were supported financially by Australia's grape growers and wine makers through their investment body the Grape and Wine Research and Development Corporation (GWRDC), with matching funds from the Australian Government. We thank the GWRDC, the University of Adelaide and IPAS for supporting this project. Tanya Monro acknowledges the support of an ARC Federation Fellowship.

Disclaimer: This publication may be of assistance to you but the authors and their employers do not guarantee that the publication is without flaw of any kind or is wholly appropriate for your particular purposes and therefore disclaim all liability for any error, loss or other consequence, which may arise from you relying on any information in this publication.

Copyright Statement: This work is copyright. Apart from any use permitted under the Copyright Act 1968, no part may be reproduced by any process without written permission from the University of Adelaide.

Table of Contents

Section number	Section title	Page
1	Abstract	4
2	Executive Summary	4
3	Background	7
4	Project Aims and Performance targets	10
5.1	**Introduction**	11
5.2	**Methods**	13
5.2.1	Chemical reagents	13
5.2.2	Apparatus	14
5.2.3	Experimental Approach	16
6	**Results and Discussion**	17
6.1	In-cuvette results	17
6.2	In-fibre results	31
6.3	Other Related Progress	37
7	**Outcomes and Conclusion**	38
8	**Recommendations**	38
9	**Appendices**	41
9.1	Communication	41
9.1.1	Smart Bungs Progress report	41
9.1.2	Article	47
9.1.3	Advertiser article	48
9.1.4	Poster	50
9.2	Intellectual Property	51
9.3	References	52
9.4	Staff	54
9.5	Additional Data	55

1.Abstract

Levels of sulfur dioxide (SO_2) are vital during secondary fermentation and throughout the maturation of wine to prevent oxidation and to protect the wine from spoilage as it develops. The current methods for monitoring SO_2 concentration utilise relatively large (up to 100 mL scale) samples and require regular human intervention. What is needed is a system that can monitor SO_2 in real time using low volumes and is sufficiently low cost to be embedded within every barrel. The objective of this investigation was to demonstrate the 'proof of concept' for such a device. This investigation has shown that microstructured optical fibres can be combined with a known colourimetric reaction to detect a quantifiable change in spectral absorbance that is linearly related to the concentration of SO_2 and that operates on nano-litre scale samples. With further work needed on the microfluidics and additional testing with real wine samples, a 'smart bung' could be developed to be used within wine barrels.

2.Executive Summary

Australia is known around the world for its excellent wine. Throughout the fermentation and maturation stages of wine production, several important parameters must be monitored and controlled to ensure both quality and reduction in product spoilage. One of these variables is the sulfur dioxide concentration (SO_2).

SO_2 is vital for producing good quality wines as it is not only used as an anti-oxidant, but it also has excellent antimicrobial properties. The current method for monitoring SO_2 requires samples to first be removed from the barrel and tested using a lengthy several step process which not only takes time, but also large volumes and with a requirement for opening the barrel with possible exposure to air. The result of this analysis is limited, providing the winemaker with just an indication of the state of the wine at that specific time point and provides no information about the path taken to get to this point. Additionally, due to time and money constraints, not all barrels are regularly tested. This means that any problems that occur in the untested barrels such as spoilage may impact in terms of overall blended wine quality and a downgrading of the wine and consequently a reduction in income.

The ultimate objective of the "Smart Bungs" project was to design a bung embedded with optical fibres which can be used to test several important parameters in near real time so that winemakers can constantly monitor the wines throughout the entire wine production process. This would allow the

winemaker to take immediate action to remedy any potential problems before the barrel becomes unsalvageable. The integration of the optical fibre based system into the bung would also allow wine samples to be extracted directly from the barrels and avoid the human contact, time and exposure to air; which occurs using existing testing methods. It would also be possible to embed a bung into every barrel so that every single barrel could be monitored individually rather than periodically testing a representative sample.

The optical fibres utilised in this system are known as microstructured optical fibres (MOF), which contain a solid glass core surrounded by a region containing holes that run the length of the fibre. When light is launched into the core of a MOF, a fraction of the light that is guided by the core spreads into the surrounding holes. When immersed in a liquid sample, these holes fill with very small volumes of sample where they can interact with any light within the fibre. This process allows us to utilise this system to detect and quantify any spectrophometric changes in the samples by either investigating the absorption or emission of light at certain wavelengths. Figure 1 illustrates this technique.

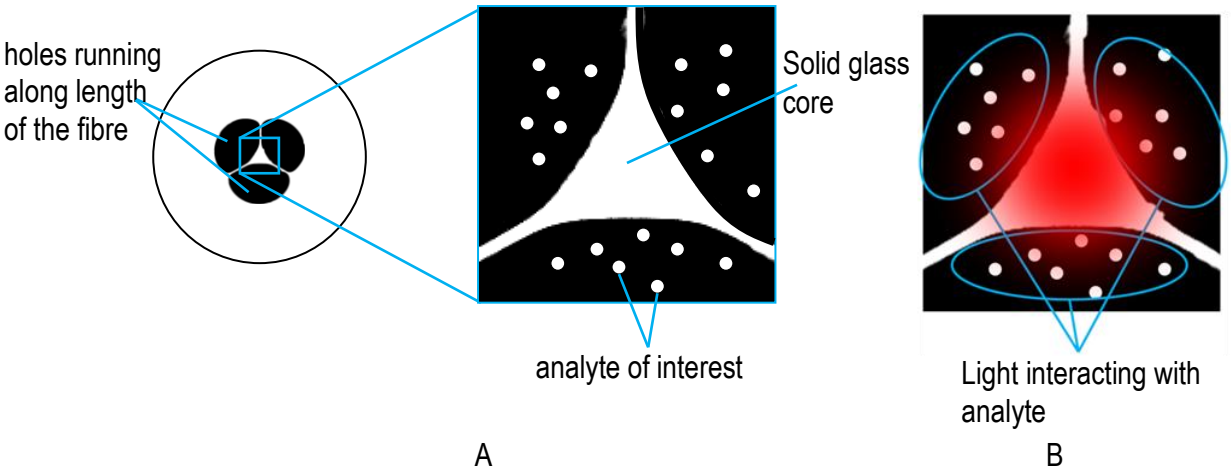


Figure 1: A: Cross section of the microstructured fibre with the detail of the core and analyte filled in the holes; B: Red light being launched into the fibre, where some of this light can interact with the analyte.

There are many advantages of the MOF system but the standout features are their very low volume requirement and that they can be used remotely and autonomously. Additionally, the core size can be tailored to ensure the interaction of light with the sample to achieve detection is in the desired range.

This pilot study aimed to demonstrate a practical implementation of the smart bung concept and the ability of this new concept to determine the concentration of free sulfur dioxide (SO_2) in model wine in a

rapid and non-intrusive manner. Sulfur dioxide is introduced to wine in the form of sodium or potassium metabisulphite. Upon addition, the metabisulphite forms pH dependent speciation (collectively termed 'sulphites') as either molecular sulfur dioxide (SO_2), bisulfite anion (HSO_3^-) or sulfite anion (SO_3^{2-}). At the pH of wine the majority of added sulphite is present in the form of bisulfite.

Two values are usually quoted for the concentration of sulfites in wine, the 'free' and 'total'. When sulfites are added to wine, a portion will bind both reversibly and irreversibly to other compounds within the wine; whilst the remaining exists in the 'free' form. It is the sum of these bound sulfites and free sulfites that defines the total sulfite concentration.

Early stages of this investigation focussed on identifying a sensor molecule that would cause a quantifiable change in a spectral property and also be selective (or reasonably selective) for SO_2. There are two options for utilising an analyte with MOFs. The first is to surface functionalise the MOFs internal structures within the holey regions so that analytes can be directly captured. When the sample is drawn into the fibre it reacts with the functionalised surface and results in a detectable change *in situ*. During the period of this grant, work on other projects within IPAS successfully demonstrated proof of concept of this surface-functionalised optical fibre approach to chemical sensors, and both hydrogen peroxide and aluminium ions have now been detected using this approach. The second approach is to pre-mix the analyte and sample, and then to load them into the optical fibre. This can either be done in cuvettes, or, if lower samples volumes are required, using a microfluidic mixing approach to mix relatively small volumes of sample and analyte. The second approach was employed for this work to enable rapid progress to be made in the demonstration of this sensor prototype (since it does not require the development of specialised surface functionality and chemistry).

Early work identified a fluorophore (fluorescing compound), Rhodamine 6G, which the literature proposed could be de-activated upon exposure to SO_2. While initial trials using this fluorophore were promising, when this system was trialled in a 'model wine' solution (10% ethanol in saturated potassium bitartrate solution), the Rhodamine 6G was quenched not only by the SO_2, but also by tartaric acid. For this reason we decided that this fluorophore was unsuitable for the intended purpose.

The next compound that was investigated was Pararosaniline (hydrochloride). A well-documented reaction exists between pararosaniline, formaldehyde and SO_2, which is a standard method used to

monitor SO_2 in beer and other food products. A working solution was made, mixing acidified pararosanaline with formaldehyde, producing a light purple solution. Upon exposure to sulfites, this light purple solution develops into a deep purple solution. The depth of colour is dependent upon the concentration of sulfites in solution and hence can be quantified using absorption spectroscopy. A linear relationship between sulfite concentration and absorption was established up to (and in excess of) 60 ppm of sulfites in solution.

The reaction was first investigated using bulk samples in cuvette. The results showed a maximum absorbance (peak) between 545 nm and 560 nm, which was dependent upon the concentration of sulfites in solution. The results indicated that a linear relationship could be achieved if the ratio of pararosaniline : sulfites was greater than approximately 1:1.5 and that solutions reached their maximum absorbance within 10 minutes of mixing.

The second phase of the investigation involved testing the system using a MOF. Premixed solutions of PRA, formaldehyde and sulfite solution were filled into a MOF and a 532 nm laser was launched into the core. The data showed that a linear relationship between absorbance and SO_2 concentration could be achieved using this fibre based system and that these results were comparable to those found by the cuvette method.

We have shown that this novel fibre-based sensing system can detect and quantify changes in sulfur dioxide concentration. With further development of a microfluidic mixing device to form a prototype device and further testing with red and white wines, we believe that this method could be developed into a “smart bung” that is able to remove, react, detect and quantify the concentration of SO_2 directly from a barrel in an inexpensive, quick and easy manner.

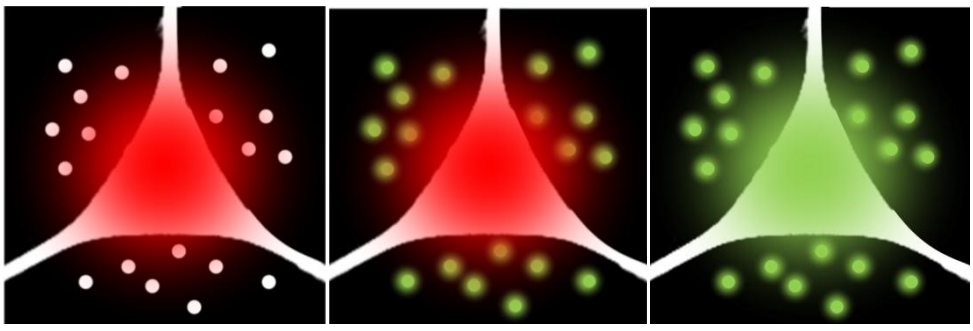
3.Background

There are many situations that can lead to the spoilage of a wine and these can occur during any of the stages of wine making from fermentation to maturation and storage. The ability to constantly monitor key indicators in the wine is paramount to achieving the desired excellence of the final product. Currently winemakers assess the quality of their wines by sampling from a representative group and analysing the samples in a laboratory. This type of testing requires time and money as well as the requirement of opening the barrel to remove a sample and hence exposing the contents to air. A joint

project between Professor Dennis Taylor (Chair of Oenology, SAFW) and Professor Tanya Monro (Chair of Photonics and Director of IPAS) aims to adapt and extend recent developments in optical fibre sensing to allow real-time monitoring of wine quality.

This real-time monitoring may be performed with what we have termed as a 'smart bung'. The smart bung would essentially be the hub for real-time sensing of numerous key parameters. This new technology will allow a winemaker to monitor their wine (on site or remotely), in a closely controlled manner that will act as an early warning system for potential spoilage or other problems. In consultation with an industry reference group, five parameters were initially identified as key parameters for constant monitoring. These were: free SO_2, *Brettanomyces* faults as evidenced by 4-ethylphenol, alcohol/sugar, malic acid and temperature. A smart bung would potentially contain a special type of optical fibre(s) through which the different parameters would be monitored quickly and in an inexpensive manner.

IPAS has an international reputation for its research in the area of liquid sensing using microstructured optical fibres (MOFs). These specific types of fibres contain a solid glass core that is surrounded by micron-scale air holes, which run along the length of the fibre. When light is launched into the fibre a portion of the light emerges into these holes where it is available to interact with any liquid within. It is this mechanism that will enable a 'smart bung' to sense changes in these key winemaking parameters. If the liquid that fills the holes is able to trigger a chemical change that can be detected spectrophotometrically, then it may be detected and quantified by investigating the absorption or emission of light at certain wavelengths. See Figures 2 and 3.



A B C

Figure 2: Schematic of fluorescence-based liquid sensing in microstructured optical fibre. A: Red light is launched into the core of the fibre, and some of this guided light overlaps with the holes filled with the liquid sample (in this case wine mixed with the sensing molecule); B: Liquid interacts with the light and fluorescence generated in the liquid (the fluorescence intensity depends on the concentration of the analyte); C: The emitted fluorescence is captured into the fibre core and detected at the ends of the fibre.

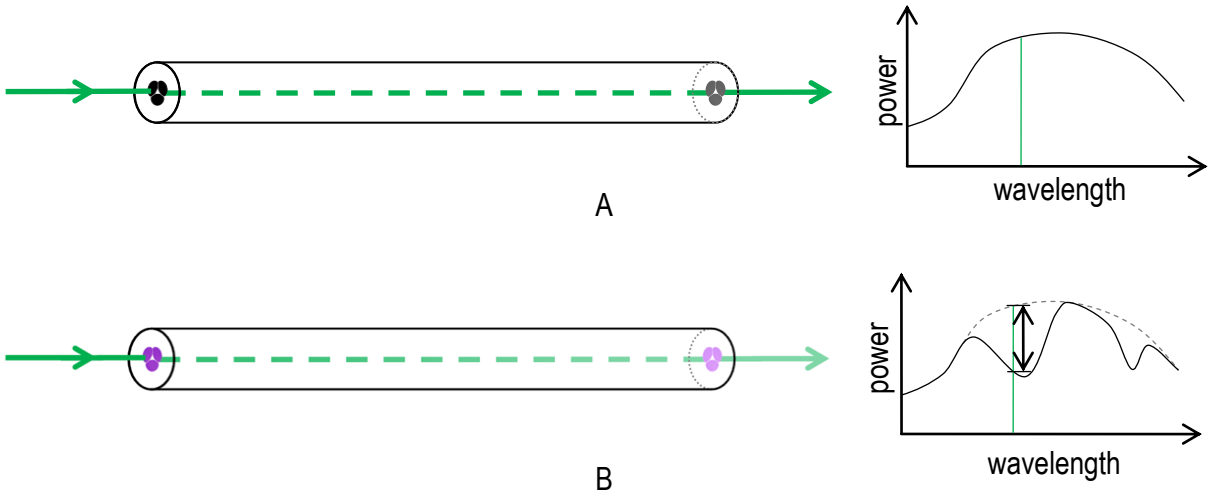


Figure 3: Schematic of absorption measurements with microstructured fibre (detection on the right hand side). A: Initial measurement with empty fibre and resulting spectrum; B: Final measurement when fibre is filled (purple liquid) and resulting spectrum. The decrease in power at a certain wavelength determines the absorbance.

To enable this GWRDC project to proceed with reduced funding (relative to the funding required/requested), it was suggested by the GWRDC that the initial stages of this 'smart bungs' project should be pared back to a single key parameter and be used to provide a 'proof of concept' for future work. The parameter chosen was free sulfur dioxide (SO_2).

SO_2 is used in wine-making processes to keep the wine fresh. Molecular SO_2 is without doubt the most important preservative/antioxidant used during the wine making process. It is also a well-established antioxidant and plays a vital role during wine storage in preventing various oxygen-induced spoilage. The potential exposure to atmospheric oxygen when barrels are opened for testing is a very real problem and is something that could be virtually eliminated with a monitoring mechanism such as the 'smart bung'.

SO_2 is added to wine in the form of potassium or sodium metabisulfite, which then undergoes pH-dependent speciation. At high pH the sulfite ion (SO_3^{2-}) is the most prominent, however, at the pH of wine (from 3.2-3.8) the main species in solution is the bisulfite anion (HSO_3^-) with a small portion available as molecular SO_2 [1]. Collectively these species are referred to as 'sulfites'. There are two concentrations of sulfites that are usually measured; the concentration of 'free' sulfites and the concentration of 'total' sulfites. When added to wine some of the sulfites bind reversibly and irreversibly to other compounds and these are referred to as 'bound' sulfites. The total sulfite concentration is the

sum of the ‘free’ and ‘bound’. This project will investigate the detection of the ‘free’ sulfites in solution with the possibility of real-time and autonomous testing as options for the future.

4. Project Aims and Performance Targets

The ultimate aim of our ‘Smart Bungs’ research is to develop a device that can be incorporated into every barrel of wine and monitor key parameters throughout the entire wine-making procedure. The aims of this project were to undertake a pilot study to demonstrate the first realisation of a ‘smart bung’ and identify a route for future development. The main aims and targets are outlined below.

Aim 1 - Demonstrate an approach to the detection of free SO_2 in a cuvette for model wine and white wine samples with the capacity to be extended to the smart bung sensing platform. The performance targets involved were:

- Finding an appropriate analyte that can be utilised for detection in model wine solution.
- Optimise the analysis technique for the concentration range required (encompassing 10-30ppm sulfites).
- Validate this system using white wine samples.

Aim 2 - Convert the bulk analysis approach into the optical fibre platform. The performance targets involved were:

- Utilising pre-mixed model wine samples to optimise the set-up for detection using microstructured optical fibres (MOFs).
- Compare results obtained in MOF’s to those obtained in the cuvette model.
- Advance the approach by performing preliminary work on the combination of micro-fluidics mixing technologies with microstructured optical fibres for future smart bung technologies.

These aims and performance targets serve to underpin a proof of concept for in-fibre detection of free SO_2 in model wine and real wines.

5.1. Introduction

Many of the faults that occur in wine occur as a result of insufficient sulfur dioxide (SO_2) and hence a sensor for SO_2 was a primary focus of this work. The affinity of SO_2 or its aqueous equivalent (bisulfite) toward certain functional groups, particularly aldehydes and other carbonyl bearing groups was exploited in order to achieve this. The first step in this project was to identify an analyte, which upon reaction with sulfites, would cause a quantifiable spectrophotometric change. Once identified, this analyte would first be tested in-cuvette (bulk) and once optimised, tested using microstructured optic fibres (MOF).

A fluorophore is ideal for this type of detector as it has the ability to be attached (surface functionalised) to the inside surface of the holey regions in the MOF, so that when a sample is drawn into the fibre it can react *in situ*.

Initial work on this project identified the fluorophore Rhodamine 6G which the literature reported exhibited a SO_2 dependent change in fluorescence [2]. The results of the testing showed that the selected fluorophore exhibited a fluorescence intensity that was linearly related to the concentration of the Rodamine 6G and could be achieved in methanol and some model wine solutions; however, the relationship was clearly linear when tested against sulfites. When the fluorescence of Rhodamine 6G was being analysed it was found that quenching by certain components within model wine was occurring (See section 9.1.1). This indicated that it was unlikely to be suitable for use in this type of system until the chemistry is further understood.

Utilising the affinity of SO_2 for aldehydes and carbonyl grounds, a literature search provided the grounds for a reaction to evaluate. A known and documented reaction exists between the dye pararosanaline, formaldehyde and SO_2. Originally this method was more commonly known for its detection of aldehydes as a Schiff base [3,4], however this method was adapted by West and Gaeke [5] for the quantification of SO_2. This reaction is also used to determine sulfur dioxide in beer [6] as well as dried fruit [7].

Pararosananline hydrochloride is an aromatic tri-amine (Figure 4A) that forms a bright magenta solution when dissolved in aqueous solution (Figure 5A). Upon acidification with hydrochloric acid the solution is essentially bleached due to diminished conjugation resulting in a pale biscuit solution (Figures 4B and

5B). The addition of formaldehyde results in initial formation of the iminium ion and affords a pale purple solution (Figure 4C, from hereon in referred to as the 'working solution'), which reacts extremely readily with sulfite to ultimately form the highly conjugated alkyl amino sulfonic acid (Figure 4D) as a rich purple solution (Figure 5D, from hereon in referred to as the 'coloured solution'). Consequently, the absorbance of visible light by this solution will be dependent upon the concentration of sulfites in this solution.

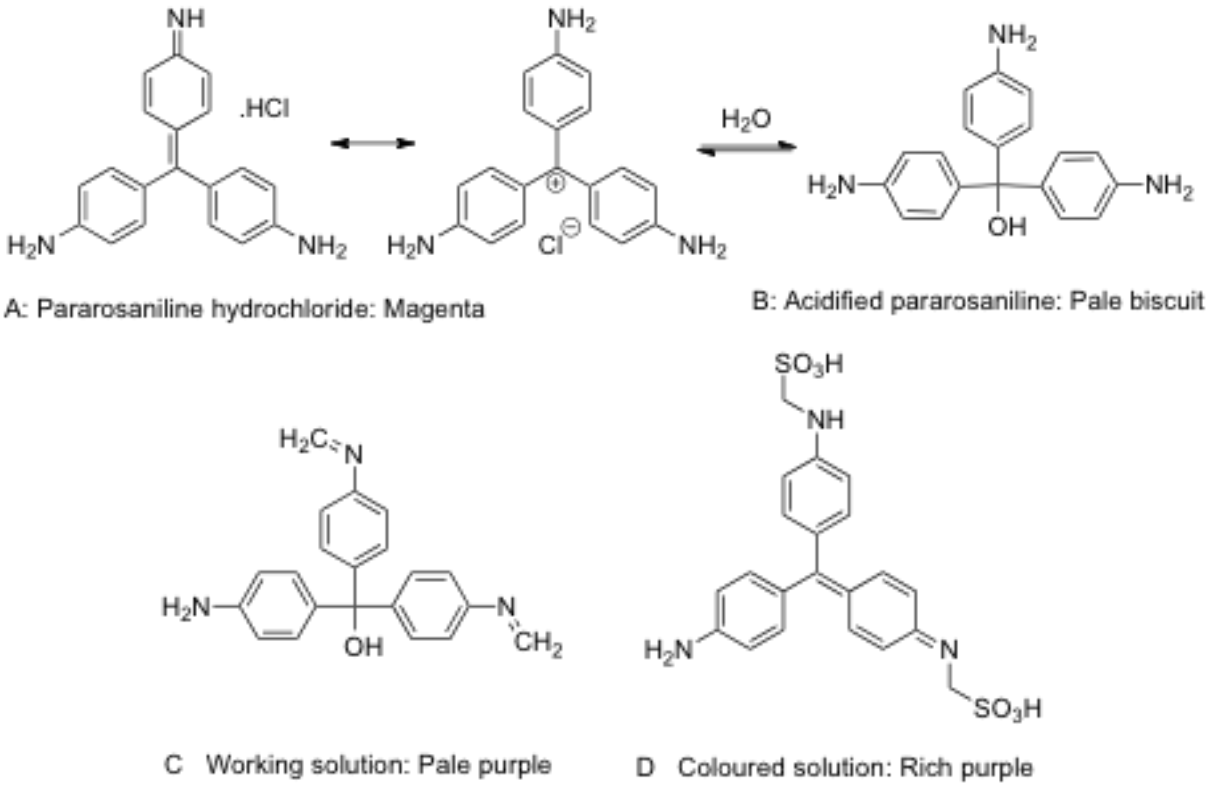


Figure 4: Chemical structures of the four compounds produced throughout the Pararosaniline reaction. A: Pararosaniline hydrochloride; B: Acidified pararosaniline; C: Pararosaniline working solution; Sulfonic acid mixture (coloured solution) [8].

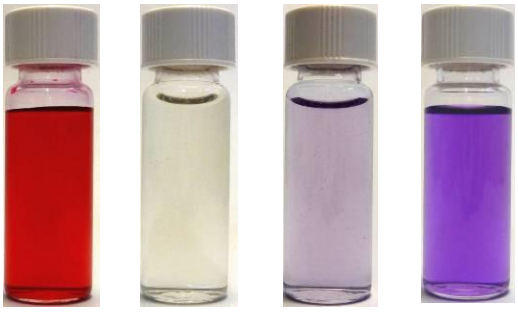


Figure 5: Solutions of the four compounds illustrated in figure 4. A: Pararosaniline hydrochloride solution; B: Acidified Pararosaniline; C: Pararosaniline working solution; D: Sulfonic acid mixture (Coloured solution).

With a colourmetric reaction such as the PRA reaction, the way in which a fibre-based sensor will operate will need to be slightly different. As this is an absorption based measurement the most appropriate way to use MOFs would be to use a microfluidic mixing approach whereby the sample and the analyte are mixed prior to filling the fibre. In the ultimate device, the mixed sample/analyte solutions could be flushed through the fibre, enabling multiple successive measurements to be made in the one sensor, however, the development of such a probe was beyond the scope of this pilot study.

5.2. Methods

5.2.1 Chemical reagents

All chemical reagents were of high purity grade with no further purification required. Millipore water (Elix® Advantage system, France) was used for the experiments.

Pararosaniline solutions

Concentrated PRA stock solution was used to make PRA working solutions. Working solutions contained pararosaniline hydrochloride, hydrochloric acid (HCl) and formaldehyde in the molar ratio of 1:1255:125 respectively [9]. The concentration of PRA in the working solution was adjusted in order to maintain linearity in absorption measurements over the desired sulfite range.

For instance, a working solution with PRA concentration of 4.68×10^{-4} mol/L in 25 mL contained 3790 µL of concentrated PRA stock (3.088×10^{-3} mol/L PRA), 1439 µL of 32% HCl and 189 µL of 36% formaldehyde solution; the volume would then be completed to 25 mL with water.

The concentrated stock PRA was made by dissolving pararosananiline hydrochloride (Sigma Aldrich) into a 10% ethanol in water solution so that the final concentration was approximately 3.088×10^{-3} mol/L.

Model wine solutions

Model wine solutions were made via dilution from a stock model wine solution. The stock model wine solution contained sodium metabisulfite dissolved in 10% ethanol in saturated potassium bitartrate (>5.7 g/L in water) solution. The purity of the sodium metabisulfite had previously been determined to be ~92% and the final concentration of sulfites in the stock was adjusted accordingly.

The required volume of model wine stock solution was pipetted into volumetric flasks and topped with 10% ethanol/saturated potassium bitartrate (>5.7 g/L in water) solution to ensure that the resulting solutions were in the range required.

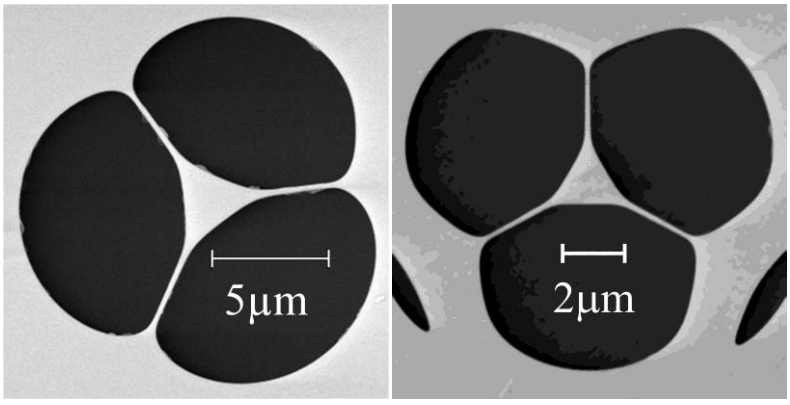
5.2.2 Apparatus

In-cuvette absorption measurements

A Varian Cary 5000 spectrophotometer was used for all in-cuvette absorbance measurements. Measurements utilized double beam mode at full slit height in the UV-Vis mode through either quartz or plastic cuvettes (4 mL internal volume) with a 1cm path length. Varian UV Scan application software version 3.00 was used for single point data acquisition; scanning kinetics software was used when absorbance was measured as a function of time. Water was used as the baseline correction and a heated cell block was used to control the temperature during analysis.

Fibre

The microstructured optical fibre (MOF) used for this study was fabricated in-house from F2 glass, a commercially available lead-silicate glass, using the billet extrusion technique [10]. Two different fibres with different core sizes were utilised. Figure 6 shows a scanning electron micrograph (SEM) of the core of the fabricated fibres. The first fibre (Figure 6A) had an outer diameter of 160 µm (not illustrated) and a core diameter of 2.1µm and the second fibre (Figure 6B) had an outer diameter of 130 µm and a core diameter of 1.39 µm. Note scale represented on each micrograph.



A B

Figure 6: Scanning electron micrograph (SEM) of the cores of the fabricated F2 fibres used for this study. Note that the full fibre diameter is not represented in these images, however a scale bar to indicate the size.

Other equipment

The schematic of the experimental set up for fibre measurements is shown in Figure 7A. The two ends of the fibre were placed in fibre holders on three-axis translation stages to enable the accurate alignment of the incoming laser light into the micron-scale fibre core. The light from the 532 nm laser was attenuated by a neutral density filter and launched into the core of the fibre using a 60x objective lens. The transmitted light was focused at the pinhole plane by a 60x objective lens. The pinhole size was set to let the light from the fibre core to pass through to the detector, which was connected to a power meter.

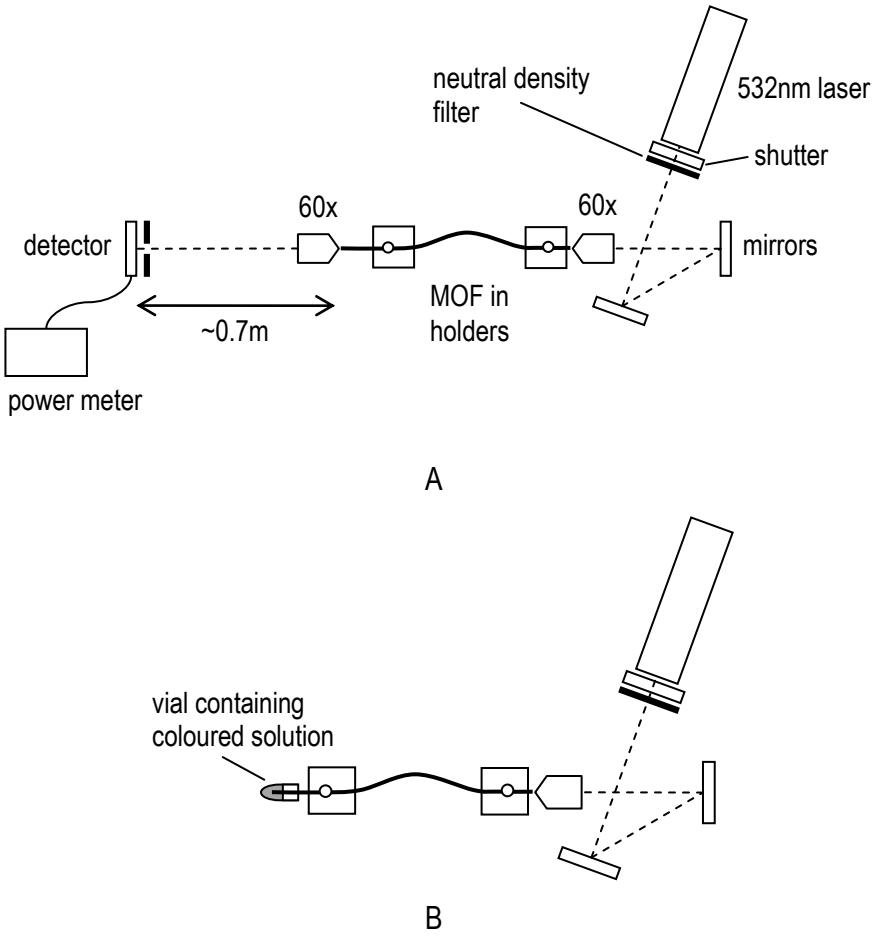


Figure 7: A) Experimental set up for the in-fibre absorption measurement (not to scale). B) Schematic of the filling phase of the absorption measurement.

5.2.3 Experimental Approach

Several different tests were performed with the bulk pararosanaline solutions in order to investigate the reaction and its possible use within liquid samples including model wine and several real wine samples.

Testing included investigating the importance of PRA concentration, the effect of ethanol percentage and tartaric acid (potassium bitartrate), temperature and wavelength dependence on the capacity to respond to the sulfite concentration in the wine sample was evaluated.

In-cuvette measurements

When performing in-cuvette measurements dilutions were required as the absorbance of neat solutions was too high for the spectrometer to analyse. When assessing the absorbance as a measure of time (for instance measuring the development time) samples were mixed directly in-cuvette with a small magnetic stirrer. Absorbance measurements were taken at set time points to observe the trend. When taking a single absorbance measurement, solutions were added to the cuvette and allowed to develop without mixing.

Unless stated otherwise, each sample was made by adding 300 µL of working solution, to 300 µL of sulfite solution and topped to 3 mL with water. Absorbance measurements were analysed as outlined above.

In-fibre measurements

The solutions used in the cuvette experiments were also used for the in-fibre measurements. These measurements were performed on the same day as the cuvette measurements using the same solutions. Equal volumes of the PRA stock solution and the model wine solution were pipetted into a PCR tube with a hinged lid, mixed and left to develop. The development time was a minimum of 15 minutes, and was up to 1 hour, not including the fibre filling time. Please note that analysis using the MOFs used here did not require dilution of the coloured solution. The reason for this is that the MOFs that were selected had relatively large core sizes, and thus the fraction of the guided light located in the wine was relatively small, and thus the absorption of the guided light due to the coloured solution was relatively weak. This is an advantage because it means that the wine may be tested without dilution.

For each absorbance measurement, a piece of fibre was cleaved and put on the fibre holders and held in place with magnets. Approximately 2cm of the fibre on the filling end was left protruding from the edge of the fibre holder (Figure 7A). The translation stage was adjusted such that the light was launching into the core of the fibre. The coupling was then optimised by focusing the transmitted light at the pinhole plane and launched onto the detector and adjusting the translation stage on the laser end to

obtain the highest power. The power was recorded over a 30 second period. The objective from the filling end was then removed, and the vial containing the mixed solution was put in a holder to allow the fibre tip to be immersed in the liquid without moving to maintain the fibre alignment (Figure 7B). The fibre was left to fill via capillary forces for a set time before the vial was taken away. The objective was then replaced on the filling end and refocused on the pinhole plane as before. The power was recorded over a 30 second period. Immediately after this measurement, the filled length of the fibre was measured under a microscope. A new fibre was used for each measurement.

The fibre lengths and filling times were different for the two different fibres used, and are summarised in Table 1. These differences in fibre length and filling time only changed the eventual filled length of the fibre. The differences in length were taken into account by calculating the absorbance per cm. Additionally, for measurements using fibre 2, the mixed samples of coloured solution were filtered with a 0.45 µm pore filter immediately before filling the fibre. This ensures that any particulates present did not interfere with the measurements, thus decreasing the spread in the data.

Table 1: Parameters that varied between measurements using fibre 1 and 2.

Fibre	Fibre length (cm)	Filling time (minutes)	PRA concentration in working solution (mol/L)	Sample filtering
1: 2.1µm core diameter (Figure 6A)	19 ± 0.2	7	7.80×10^{-4}	No
2: 1.39µm core diameter (Figure 6B)	16 ± 0.2	5	6.24×10^{-4}	Yes

6 Results and Discussion

6.1 In-cuvette results

Initial experiments were performed using sodium metabisulfite dissolved in water. Once the method was demonstrated to work, this was then performed using a model wine solution. It was important to ensure that the high concentration of tartaric acid (potassium bitartrate, KHT) in wine did not hamper the reaction as we had found was the case with Rhodamine 6G. Figure 8 illustrates a comparison between reactions of the working solution with sulfite solutions containing 10% ethanol in water and sulfite solutions containing10% ethanol in saturated KHT solution.

Initially, to test the validity of our approach, these solutions were not diluted. Equal volumes (1.5mL) of working solution (6.17 x10^{-5} mol/L of PRA) and sulfite solution were pipetted into a cuvette containing a small magnetic stirrer. The absorption spectra were run every minute for 8 minutes. The maximum (peak) absorbance values at each time point for the 10% ethanol in water and 10% ethanol in saturated KHT were plotted against development time (Figure 8).

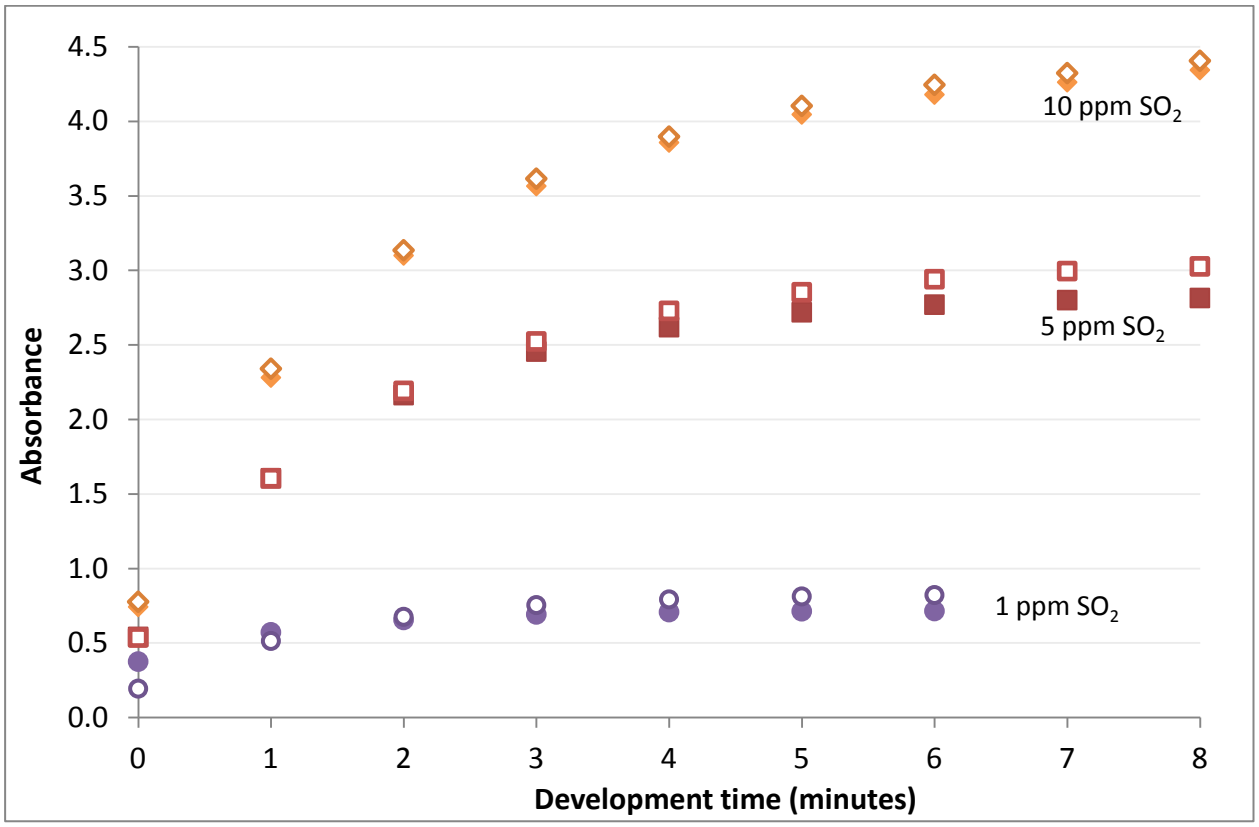


Figure 8: Comparison of maximum (peak) absorption values of model wine solutions containing 10% ethanol in water (filled data points) and 10% ethanol in saturated potassium bitartrate solution (KHT) (hollow data points) for three concentrations of sulfite solution.The points represent data from single samples.

Figure 8 shows that the presence of KHT does not appear to hamper the reaction. Although the absorbance of the coloured solutions containing the KHT appeared to be slightly higher, these results do not fall outside the expected range of experimental error. From this point forward a 10% ethanol in saturated KHT solution was used for all reactions and referred to as a 'model wine' solution.

The stoichiometry of the reaction between PRA, formaldehyde and SO_2 is not well understood. There are potentially 3 positions on a PRA molecule where the reaction could take place. Naumann, *et al*.[11] suggested that the possible end product could be a tri-substituted product while Hormann, Grossman and Fires [12] interpreted their product as being di-substituted and Pate, Loge and Wartbug [13] achieved their best results when using a 1:1 ratio of PRA:SO_2. Huitt and Lodge [14], however, claim that the spectrally active product is an equilibrium mixture of mono-, di-, and tri-, substituted pararosaniline. For this investigation a 2:1 molar ratio of sulfites: PRA was used as a basis to determine the concentration of PRA required for the desired sulfite range.

Several concentrations of PRA were investigated during this investigation and using a 2:1 molar ratio (sulfites: PRA), detection up to (and beyond) 100 ppm of sulfite was possible; however, for the investigation of free sulfites in wine the detection range between 0–60ppm was considered adequate.

Three PRA working solutions were produced with concentrations of 1.56 $x10^{-4}$, 3.12 x 10^{-4} and 4.68 x 10^{-4} mol/L. These concentrations are equivalent to sulfite concentration of 10, 20 and 30 ppm (1:1 ratio). Using the basis of a 1:2 mol ratio (PRA:sulfites), linearity in absorbance should be able to be achieved up to 60 ppm of sulfites using the most concentrated working solution.

Model wine standards were mixed with the three different working solutions as outlined above. The developed coloured solution was analysed over 150 nm (from 650-500 nm) to identify the position and value of the maximum absorbance and to investigate the peak shape. Figure 9 illustrates the maximum absorbance for each resultant coloured solution plotted against sulfite concentration.

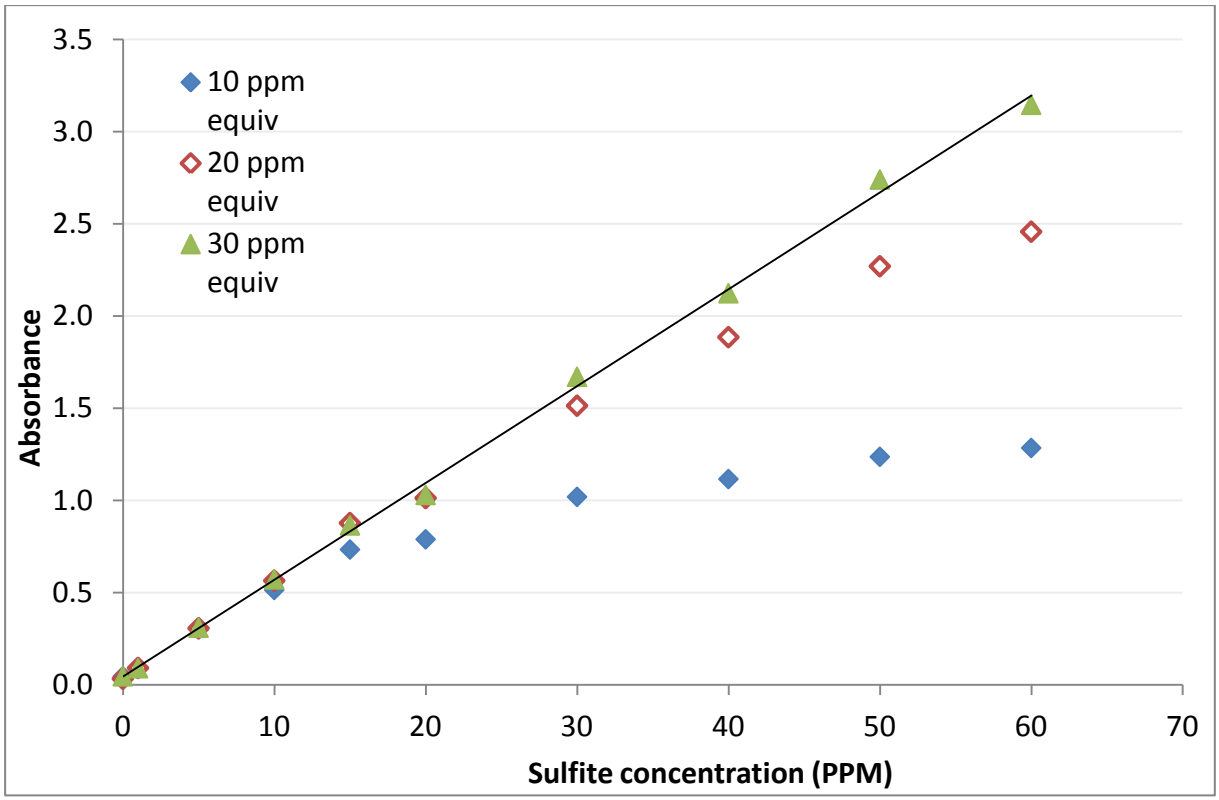


Figure 9: Maximum absorbance for three concentration of working solution as a function of model wine sulfite concentration. The points represent data from single samples.

The graph in Figure 9 clearly illustrates the importance of the stoichiometry for this reaction. It should be noted that the maximum absorbance achieved is independent of the PRA concentration in the working solution; provided that the working solution has at least a 1:1molar ratio of PRA:sulfite.

For example, it can be seen that the absorbance values for all three concentrations of working solutions are similar until approximately 10 ppm. At this point the absorbance values of the lowest concentration working solution begin to plateau out. This occurs again with the medium concentration working solution, but at a higher sulfite concentration (between 20 and 30 ppm). This graph suggests that in order to achieve good linearity over the desired sulfite concentration, a 1:1.5 ratio (or greater) of PRA: sulfite concentration should be used.

The concentration of PRA is also important in terms of shape of the absorbance spectra and hence the detection of absorbance at different wavelengths. Figure 10 illustrates this feature.

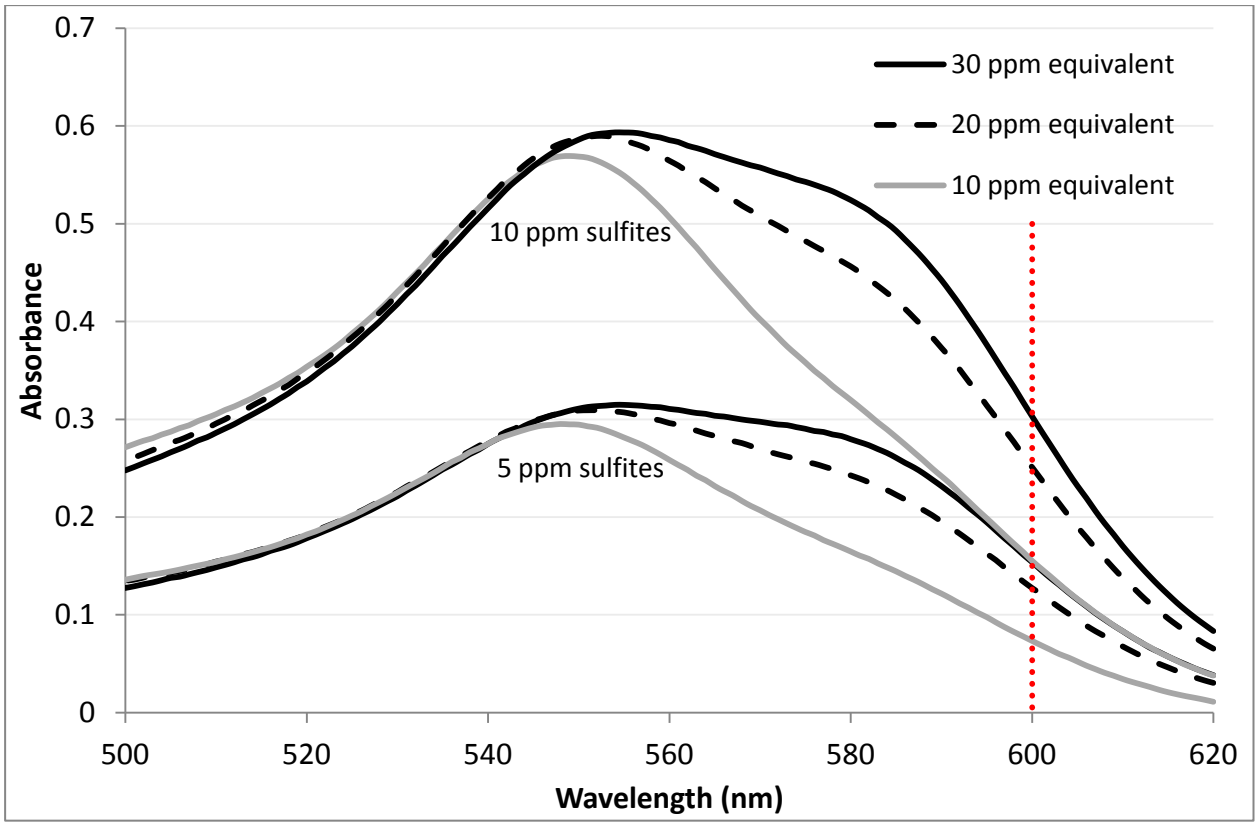


Figure10: The effect of PRA concentration on absorbance peak shape. The points represent data from single samples.

Figure 10 shows that although the maximum absorbance for each of the PRA concentrations occurs at similar wavelengths (between 548-557 nm), the absorbance values at longer wavelength are quite different. As the concentration of PRA increases, the shape of the absorbance peak flattens out, which means that detection of absorbance at these wavelengths is highly dependent on the concentration of PRA. This can be observed by looking at the absorbance values at approximately 600 nm. The absorption for a 5 ppm sulfite solution with a 30 ppm PRA solution (black line) is very similar to that of a 10 ppm sulfite solution reacting with a 10 ppm PRA solution (grey line). If one was using this wavelength to construct a calibration curve, they would have to specify the concentration of PRA used. However, this is not necessary when using wavelengths shorter than the maximum, which is an excellent finding.

In order to investigate the possibility of achieving linearity at different wavelengths a full spectrum (800-200 nm) was run using a 1:1 working solution equivalent to 40 ppm of sulfites (6.24 x^{-4} mol/L PRA) and sulfite standards up to 60 ppm (0,1,5,10,15,20,25,30,40,50 and 60 ppm). Figure 11 illustrates the full spectra for all sulfite standards. It can be seen that as the sulfite concentration increases, the peak

shape becomes sharper, which is to be expected as it is likely to be associated with the PRA working solution. As there is a need for more working solution to react with higher concentrations of sulfites, there is less available for absorption.

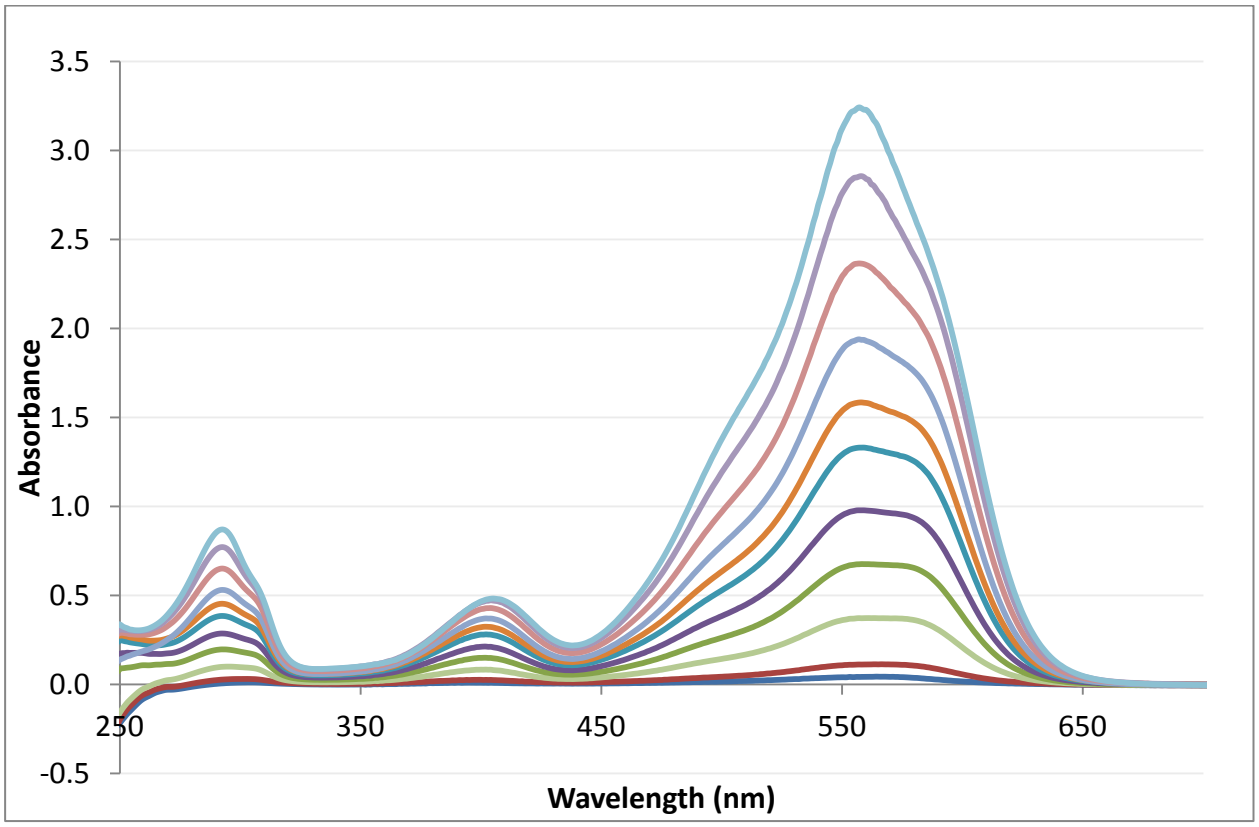


Figure 11: Full absorption spectra of coloured solution from 0-60 ppm of model wine solution. Concentration of working solution was 6.24 x 10^{-4} mol/L. The points represent data from single samples.

As shown in Figure 10; at wavelengths shorter than the maximum, the absorption appears to be quite stable and independent on the concentration of PRA. In order to be able to utilise this colourimetric reaction within a MOF, it is necessary to be able to show good linearity at the wavelength at the selected laser wavelength (532 nm). The spectra in Figure 11 were used to assess the linearity in absorbance for several different wavelengths including the desired 532 nm (Figure 12).

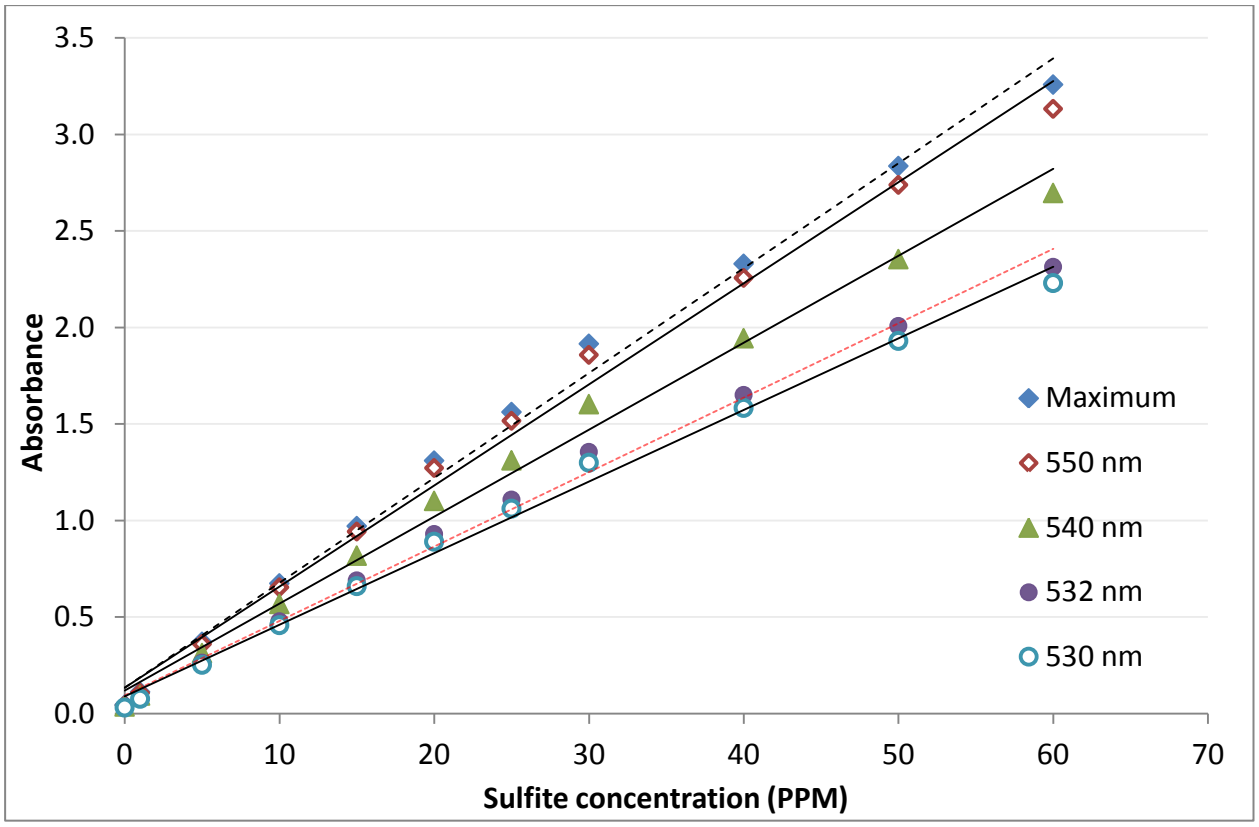


Figure 12: Effect of wavelength on the absorbance measurement of the coloured solution from 0-60 ppm model wine solution. The points represent data from single samples.

The graph in Figure 12 clearly shows that a green laser with a wavelength of 532 nm would be able to be used to determine the concentration of sulfites in model wine and possibly real wine.

One of the obvious differences amongst wines is the alcohol content. Wines can range from very low percentages of alcohol (~6%) all the way up to almost 20%. It was important to ensure that the alcohol concentration didn't affect the absorbance values for our model wine solutions.

Two different model wine solutions were made, one containing 10% ethanol in saturated KHT (standard) and one with 20% ethanol in saturated KHT. Model wine standards were made in the range of 0-60 ppm and analysed as outlined above. Figure 13 shows the maximum absorbance for each standard plotted against sulfite concentration. The two calibration curves in Figure 13 are in excellent agreement with each other, suggesting that alcohol content does not affect the absorbance of the coloured solution significantly.

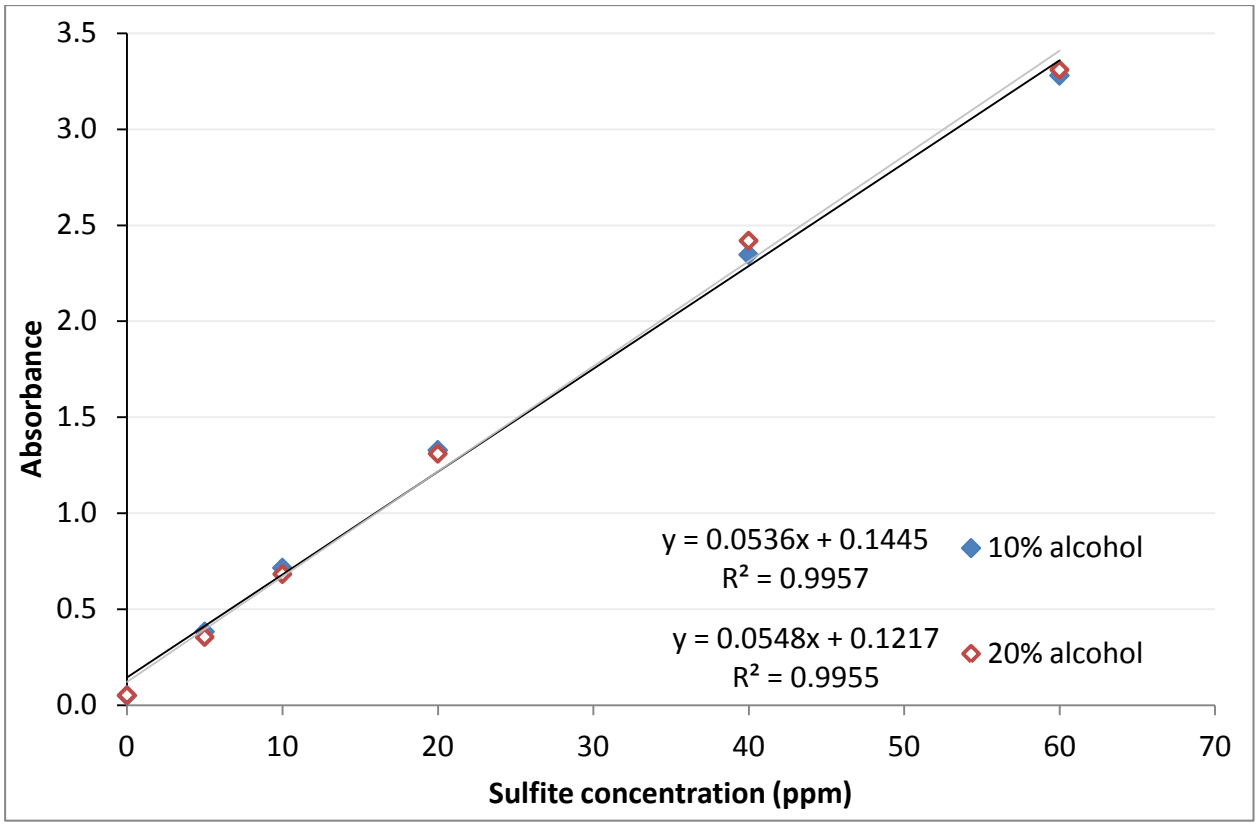
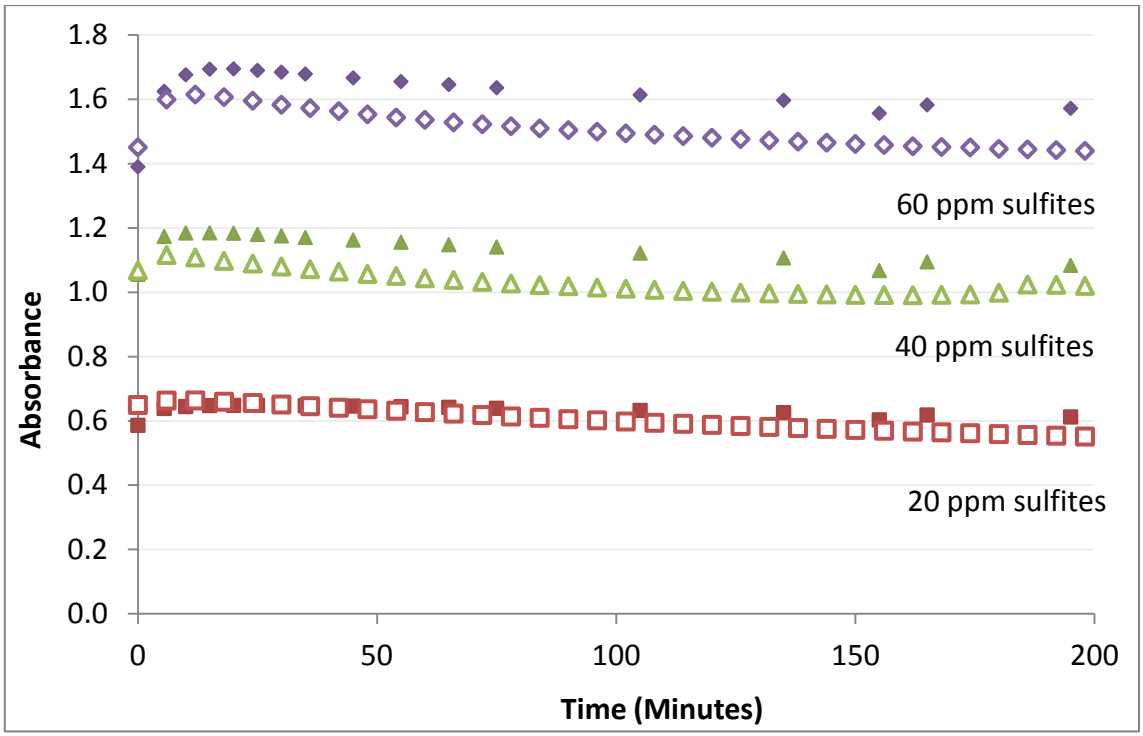


Figure 13: Calibration curves comparing model wine standards containing 10% ethanol and 20% ethanol. The points represent data from single samples.

Two other parameters that needed to be investigated were that of development time of the coloured solution and the impact on temperature. It was assumed that these two parameters were linked and hence absorbance measurements were run at specific time points and performed at 25˚C and 30˚C. Figure 14 (top) illustrates the trend in absorbance as a function of development time for three concentrations of sulfite solutions. The highest absorption measurement achieved for each model wine concentration was used to construct calibration curves for each temperature (Figure 14, bottom) It should be noted that the calibration curve extends to 100 ppm and as such the samples used in this analysis were made more dilute to keep the absorbance readings in the linear range of the UV-Vis spectrophotometer. Thus, the absorption measurements are lower than those established previously, but when the dilutions are taken into account, the values have been shown to be the same.



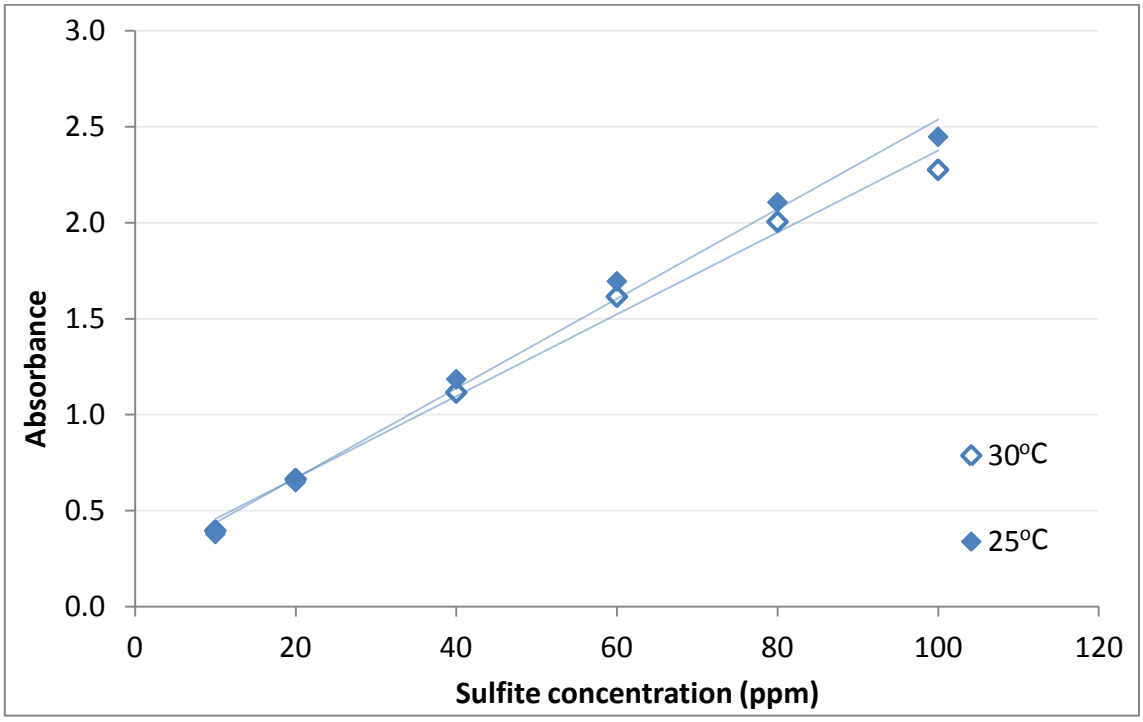


Figure 14 (top) Maximum (peak) absorbance values as a function of development time for model wine samples (20, 40 and 60ppm sulfites) at 25°C (filled data points) and 30˚C (hollow data point).(Bottom)Maximum absorbance obtained plotted against sulfite concentration at 25˚C (filled data points) and 30˚C (hollow data points). The points represent data from single samples.

The calibration curve illustrated in Figure 14 (bottom) suggests that a higher temperature actually results in a slightly lower absorbance. The reason for this is unclear. It may be possible that the peak absorbance at 30˚C actually occurred prior to the first data point acquisition in and hence the maximum absorbance value was not captured.

For the 25˚C samples, the development time where the maximum absorbance occurred was at approximately 12 minutes. At this point of the investigation, two different white wines; Wine 1 and Wine 2 (see section 9.5, Table 11) were selected and analysed using the PRA working solution. The dilution factor was the same as illustrated in Figure 14. Wines were tested in duplicate at 6 minute intervals and average absorbance measurements were taken at 20, 25, 30 and 40˚C.

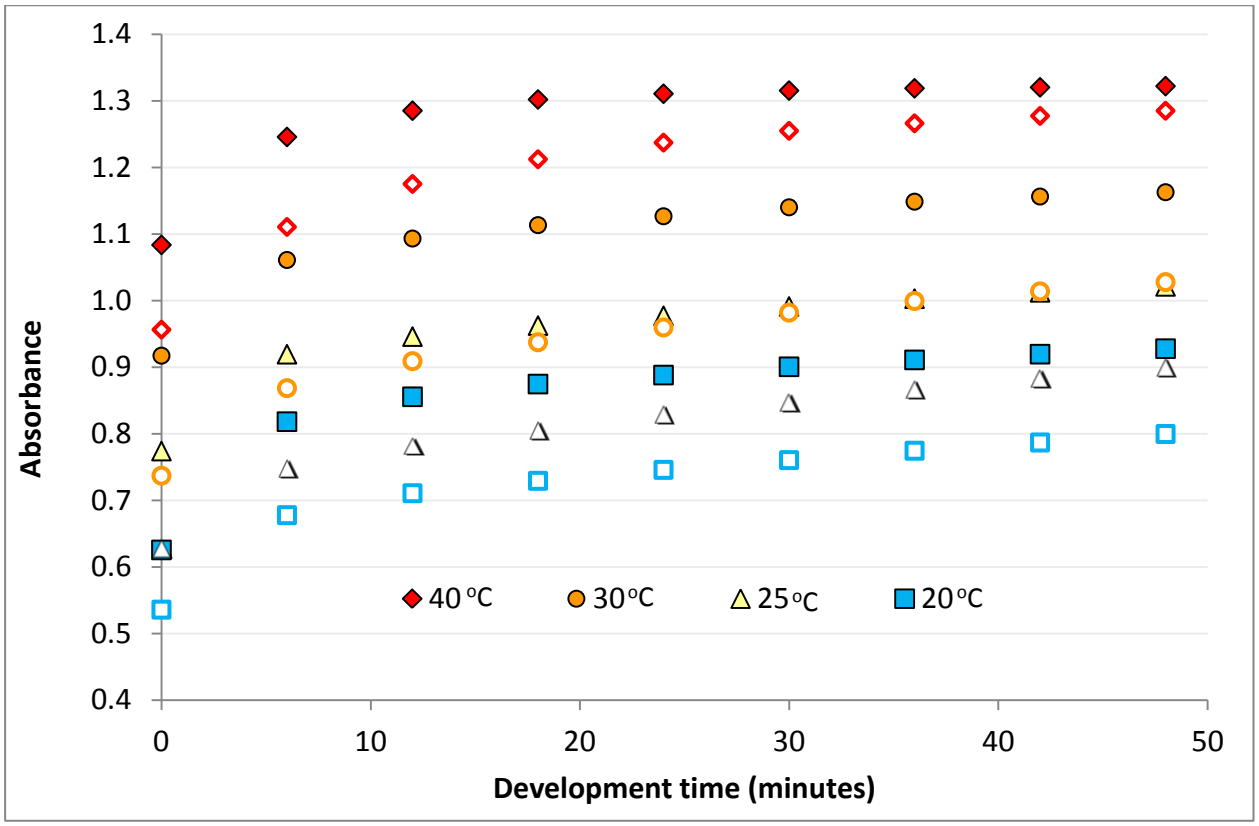


Figure15: Average absorbance of coloured solutions performed on real white wine samples as a measure of time and temperature. Filled data points represent 'wine 1' and hollow data points represent 'wine 2'. The points represent data from three separate samples which were then averaged.

As can be seen from Figure 15, real wine samples behave quite differently than model wine samples. The spectra in Figure 15 show that not only do the absorbance values continue to rise as time continues, but in addition the temperature also alters the absorption value obtained. The 48 minute absorbance measurement was used in conjunction with the 25˚C calibration curve in Figure 14 (bottom) to determine the concentration of sulfites in solution at each of the temperatures (Figure 16).

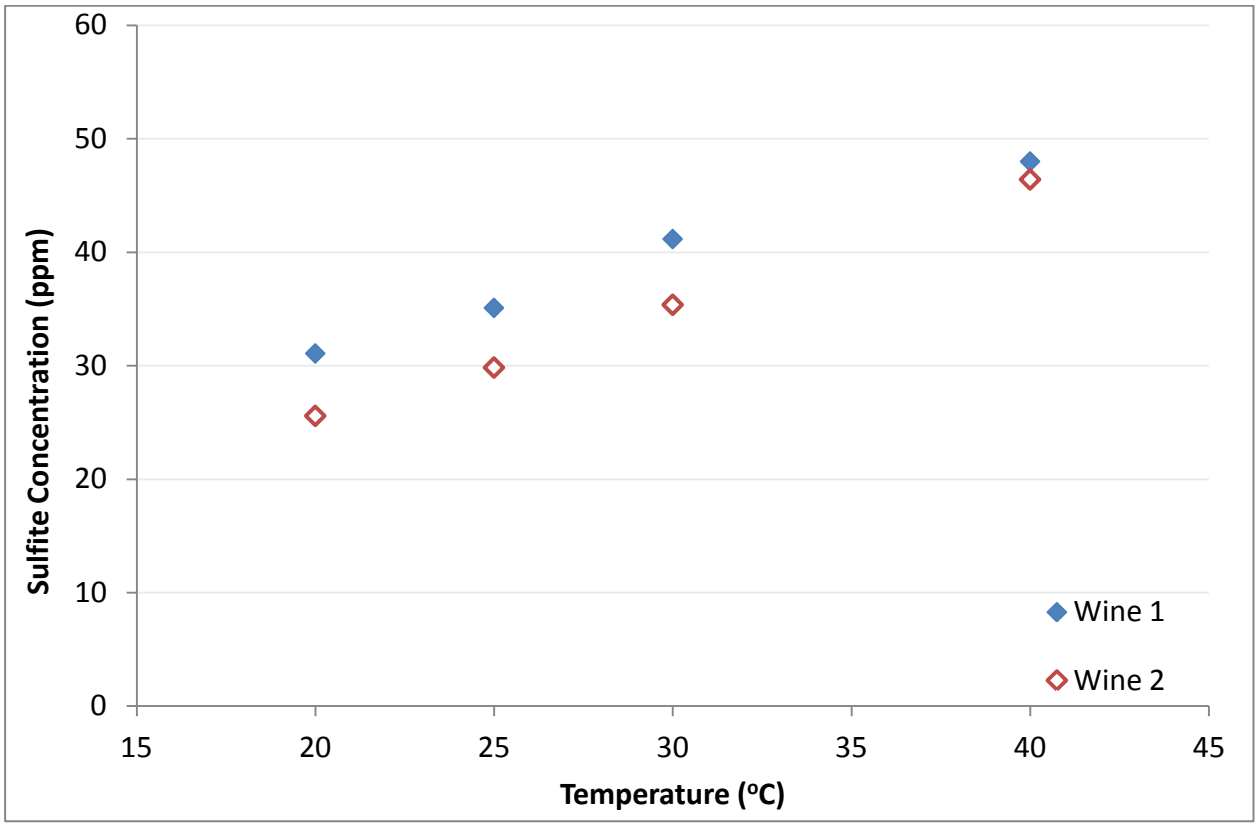


Figure 16: Temperature dependence on the measurement of sulfites in real white wine samples. The points represent data from three separate samples which were then averaged.

The graph in Figure 16 clearly shows the increase of sulfite concentration in wine samples as the temperature increases to the point where the concentration of sulfites at 40˚C is almost double than those observed at 20˚C. It is possible to explain the temperature dependence in terms of 'free' and 'bound' sulfites. As stated in the introduction, many of the sulfites introduced into wine during the fermentation period react and bind quickly with other compounds and are hence considered to be bound; however, in many cases this binding is reversible and the incidence of heat enables the reaction to be reversed. The reason for the continued rise in absorbance over time is unclear. It may be a result

of additional compounds in the wine reacting or interfering with the PRA and further investigation is required.

At this point, the optimal conditions for determining the sulfite concentrations in a 10% model wine solutions had been established. A working solution containing 6.24 x 10^{-4} mol/L PRA (300 µL) was added to a 10% model wine standard (300uL) in cuvette and topped with water (2.6 mL). A small piece of sticky tape was stuck over the cuvette (to avoid evaporation) and the coloured solution was allowed to develop for 10 minutes at 20˚C. The resultant calibration curves at both the maximum absorbance and at 532 nm can be seen in Figure 17.

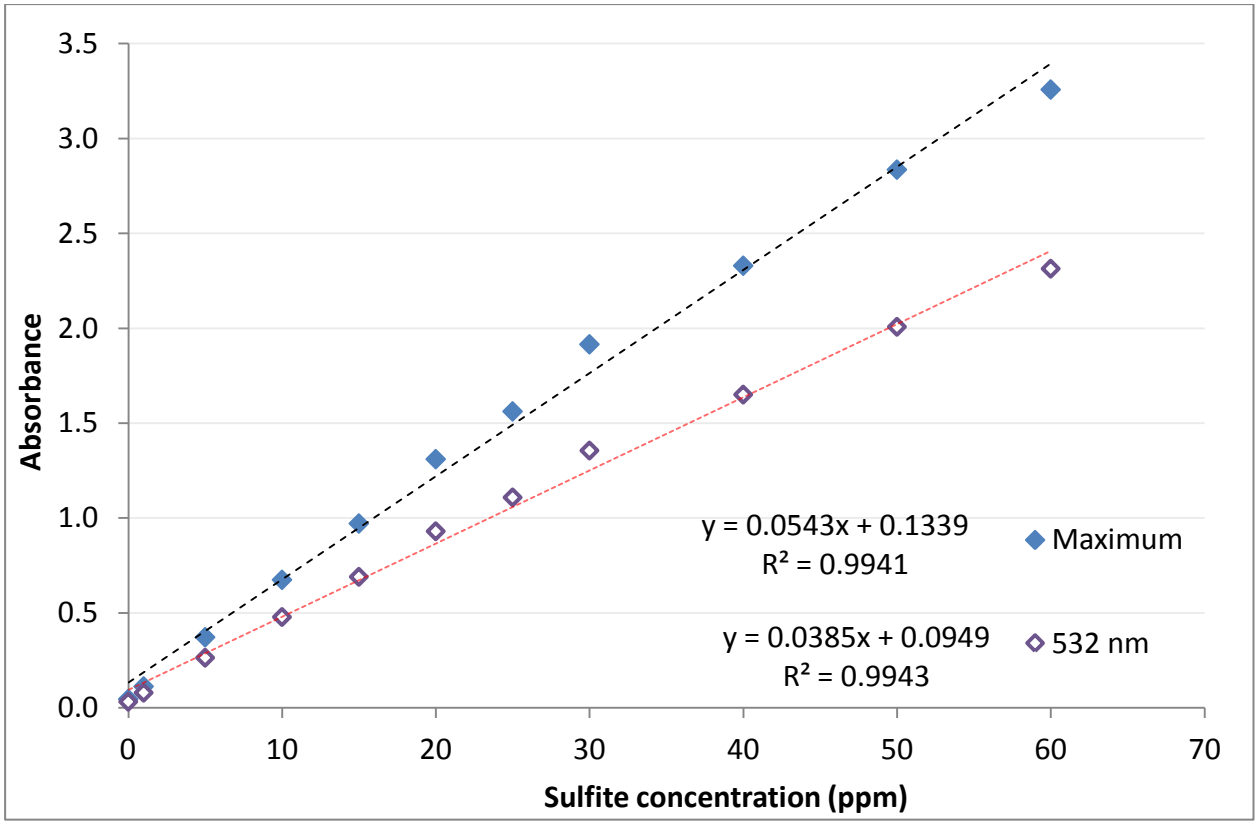


Figure17: Calibration curve from 0-60pmm at 20˚C using 6.24 x 10^{-4} mol/L PRA working solution.The points represent data from single samples.

The final piece of research required within this grant was to test the developed system using 3 white wine samples; Wine 3, Wine 4 and Wine 5 (See section 9.5, Table 13). In addition, these wines would be analysed for their sulfite concentration using the Australian industry standard (the aspiration method [15]) so that realistic comparisons could be made.

Knowing that the absorbance values were likely to continue to increase over time, absorbance measurements were made in 30 second intervals. The maximum (peak absorbance) absorbance and the absorbance at 532nm were used to determine the concentration of sulfites at each of the time points. The calibration curve illustrated in Figure 17 were then used to determine the sulfite concentration in each of the wines at each time point (19) which were then compared to the values obtained using the aspiration method to see whether a trend would be seen.

The three white wines chosen were the same variety with the same alcohol concentration (11%).

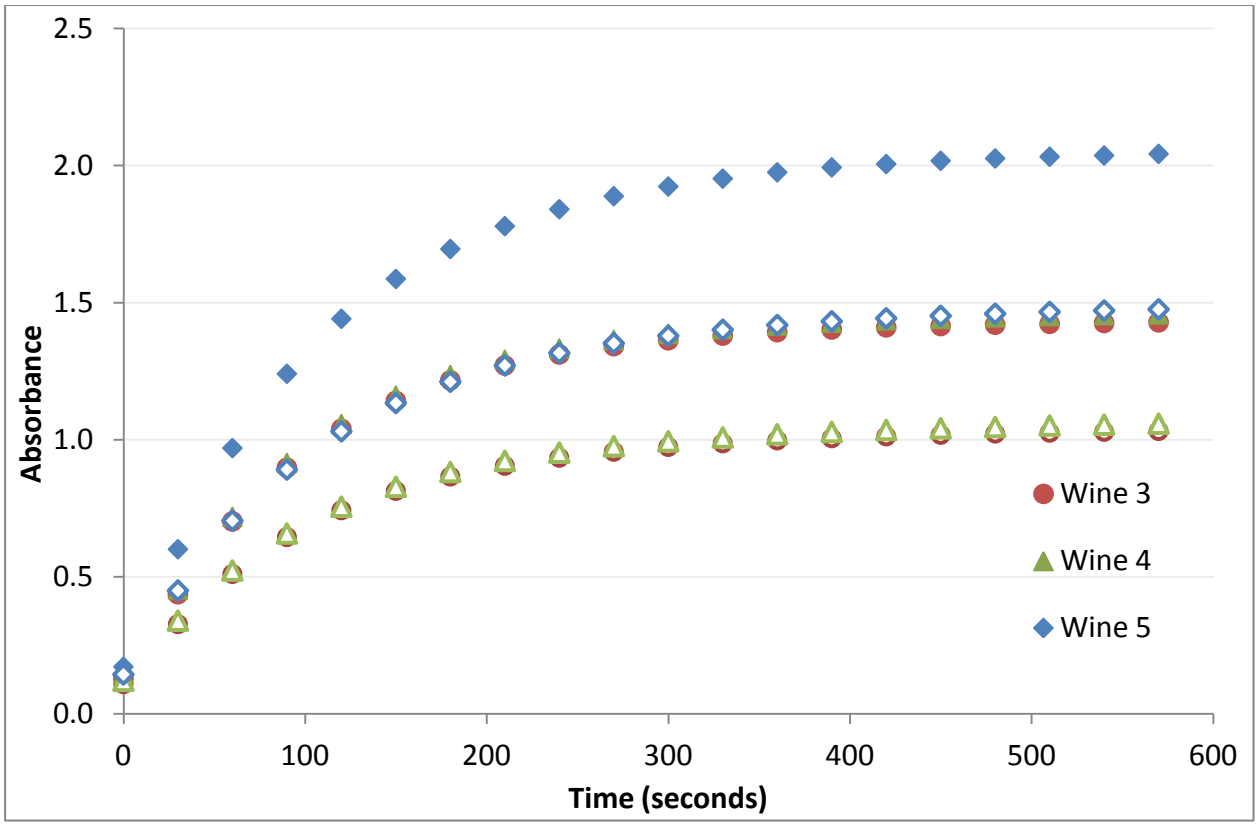


Figure 18: Maximum absorbance values (filled data points) and absorbance values at 532 nm (hollow data points) for three white wines as a function of time. The points represent data from three separate samples which were then averaged.

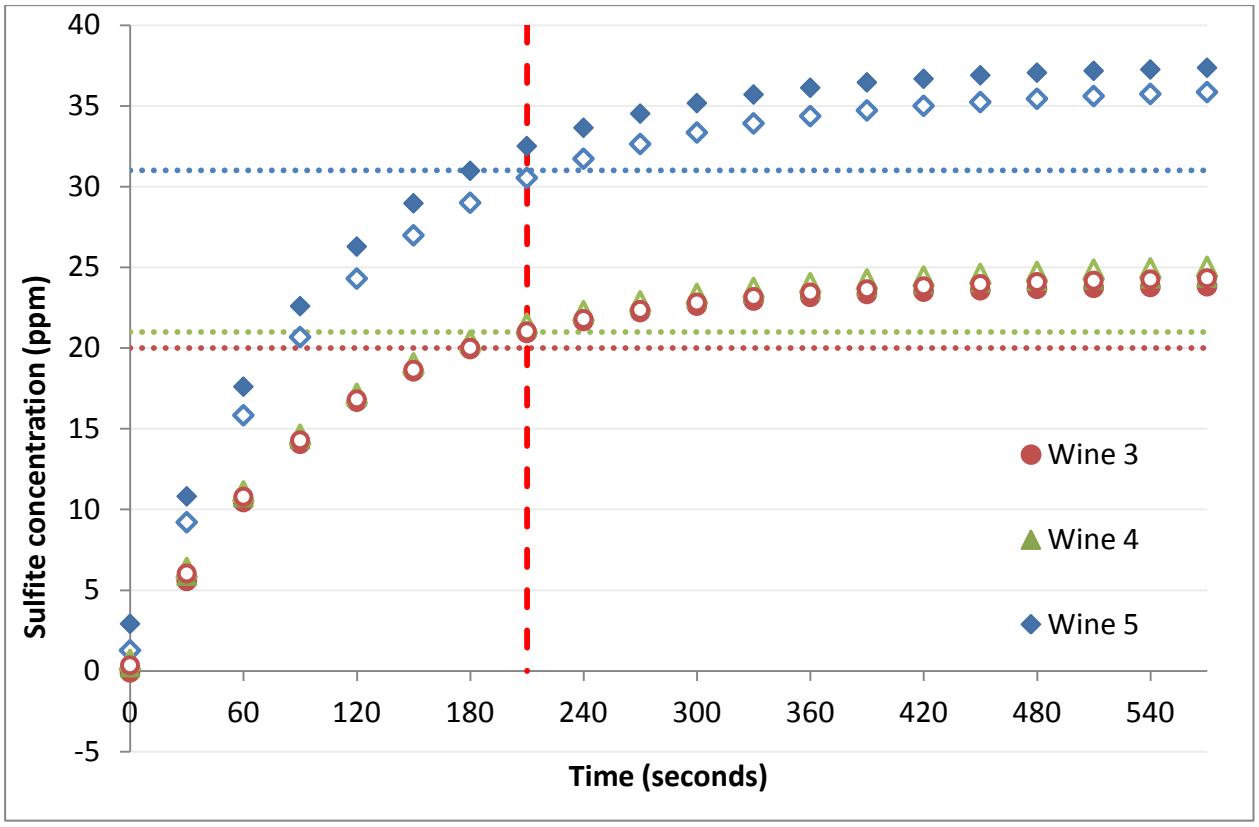


Figure 19: Concentration of sulfites utilising calibration curve at maximum absorbance values (filled data points) and at 532 nm (hollow data points) as a function of time. Horizontal dotted lines refer to the concentration determined using the industry standard method [12]. The points represent data from three separate samples which were then averaged.

Figures 18 and 19 further illustrate the point that wine is a complex medium. The absorbance values continue to increase as alluded to in Figure15. By using the two calibration curves (Figure 17) the sulfite concentration was determined at each time point. It is interesting to note that for Wine 3 and Wine 4, the concentration established at the maximum absorbance was almost identical to those established at 532 nm, however, when examining Wine 5, the concentration at 532 nm was slightly lower than that found at the maximum. It is possible that the peak shape for Wine 5 is slightly different to those of model wine solutions.

The concentration of sulfites in each of the wines was also established using the aspiration method [12]. The horizontal dotted lines in Figure 19 illustrate the average concentration of sulfites for each of the wines. What is noticeable is that these horizontal lines all intercept the PRA wine results at

approximately the same time point, and that is at approximately 210 seconds, incidentally it is also possible to divide the concentration at 570 seconds by a factor of 1.2, and still end up with values which are close to those observed with the standard method. Further testing of many more wine samples is required in order to further validate these observations.

6.2 In-fibre results and discussion

Based on the cuvette absorption measurements and methodology developed above, the research shifted to explore the potential for adapting this approach for use with the optical fibre sensing platform. The absorbance of the mixture in the fibre, A, was calculated using:

$$A = \frac{log_{10}\left(\frac{P_{unfilled}}{P_{filled}}\right)}{L}$$

Where $P_{unfilled}$ is the transmitted power of the unfilled fibre, P_{filled} is the transmitted power when it is filled with the mixture of coloured solution, and L is the filled length of the fibre (path length). According to the Beer-Lambert law, the absorbance is defined as $A = \varepsilon lcPF$, where ε is the molar absorptivity of the absorbing material, l is the path length, c is the concentration of the sample and PF is the power fraction. The power factor is the fraction of the guided light within the fibre that is available to interact with the absorbing material (i.e. the fraction of the guided light that is located within the liquid-filled holes).

For the cuvette measurements, all the light interacts with the sample so the power factor can be considered to be1. However, for a MOF with a core of > 1 micron in diameter, most of the light is confined in the core, and a small fraction spreads into the holes of the fibre which then interacts with the solution that fills these holes. The power fraction is dependent on wavelength, material type and fibre structure [16]. Fibres with a relatively large core diameter have a smaller power fraction compared to a smaller core diameter. Thus, to determine if the cuvette measurements agree with the fibre measurements, one can keep all parameters constant (same samples, path length, sulfur dioxide concentration) and compare the fibre's theoretical power fraction with the calculated power factor (the ratio of the slopes of the two calibration curves). The power factor for fibre 1 is around 1.8×10^{-3} and the power factor (which has a smaller core) for fibre 2 is 8×10^{-3}. These power factors were calculated for a step index F2 fibre filled with water and excited at 532 nm.

The calibration curve for fibre 1 was plotted and is depicted in Figure 20. Some of the absorbance readings were higher than expected – this could be because the coloured solution was not filtered, and particulates may have settled on or near the fibre core and giving incorrect (high) readings. For the range of sulfite solutions tested, good linearity is demonstrated ($R^2 = 0.9773$).

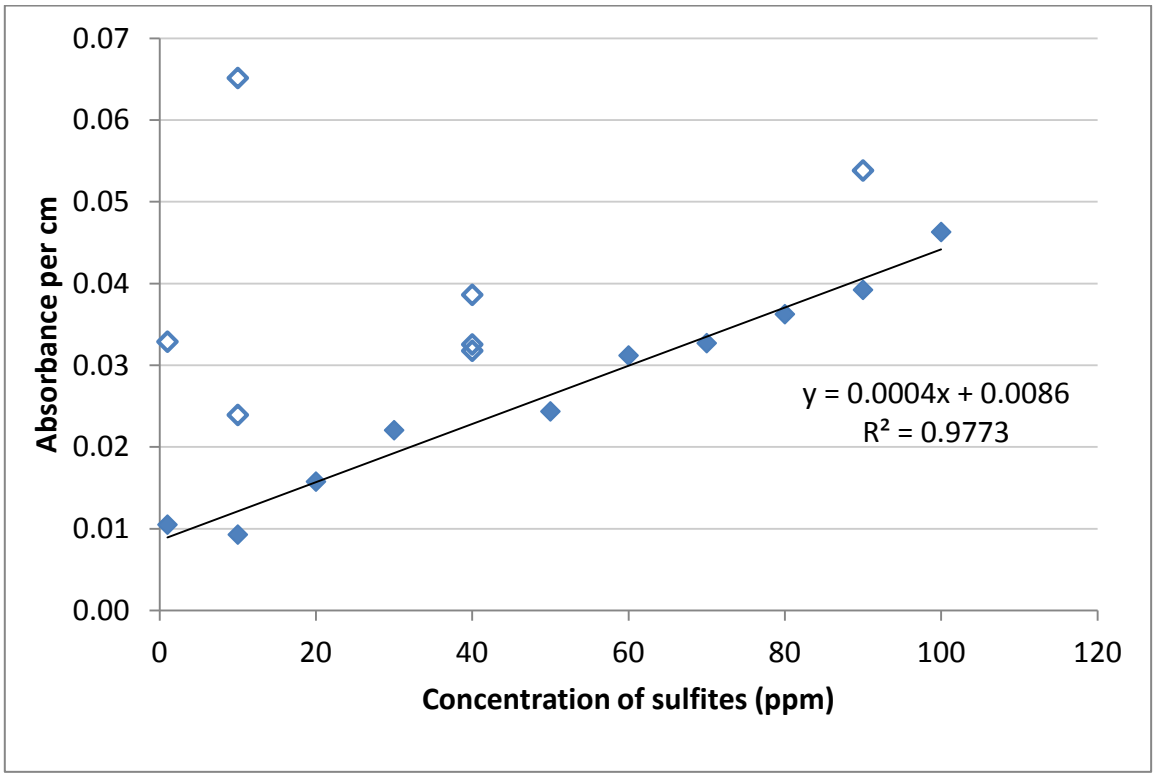


Figure 20: Calibration curve from 1-100 ppm using $7.8x10^{-4}$ mol/L PRA working solution in fibre 1. Data points not included in the calibration curve are shown as the hollow data points.

The calibration curve for fibre 2 is shown in Figure 21. Note that the range of sulfite concentrations was decreased to 40 ppm as this is the desired detection range for the winemaker. This data is much less scattered due to the filtering of the sample (consistent with the explanation that in the previous results, large particulates may have adhered to the core), and the R^2 value of the calibration curve is reasonable. As the core of fibre 2 is smaller than fibre 1, the interaction between the sample and the light is high and thus the calibration curve has a higher slope.

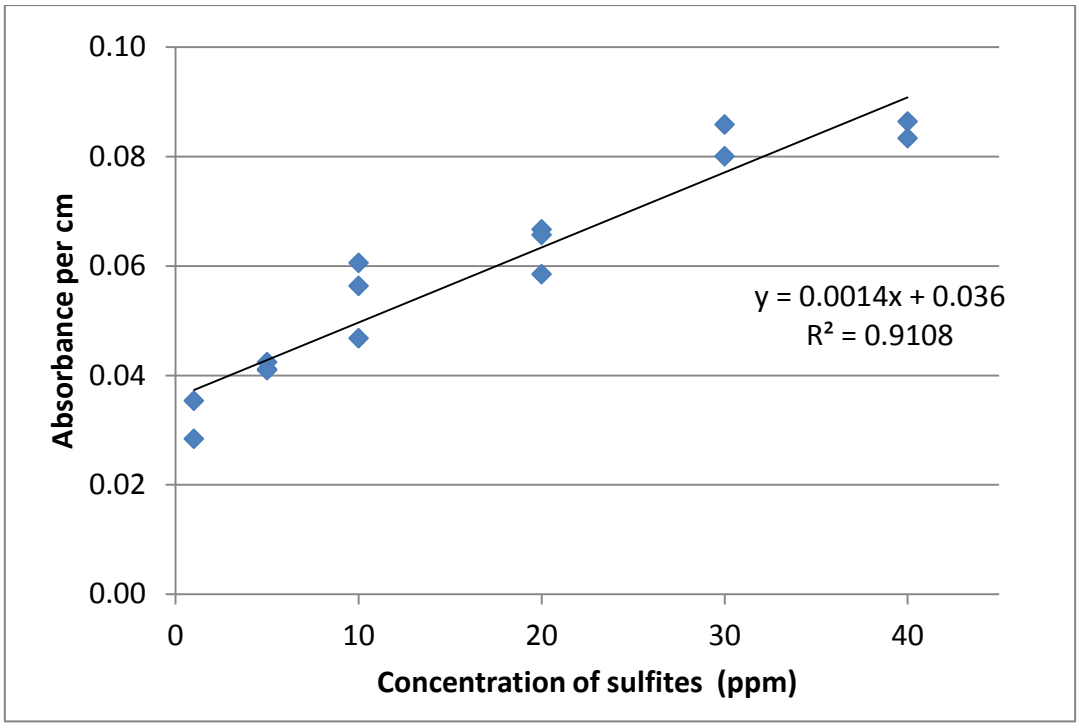


Figure 21: Calibration curve from 1-40ppm using 6.24x10^{-4} mol/L PRA working solution in fibre 2.

To allow for direct comparison between the calibration curves of the cuvette and in-fibre measurements, the slopes of the calibration curve were corrected to account for the different dilutions used in the two methods. The sulfite concentration was diluted by 2 in fibre, and by a factor of 10 in the cuvette measurements. Thus, the slopes were multiplied by 2 and 10 respectively to account for this. Table 2 summarises the comparison of the theoretical and calculated power factor. The actual power factor is smaller than the theoretical power factor (15% and 9% for fibres 1 and 2 respectively), but is still within experimental error. This shows that the results achieved in cuvette can be translated into the fibre platform.

Table 2: Comparison of the fibre power factor and ratio of the slopes. The slope of the cuvette calibration curve (0.0385) is taken from Figure 17 at 532 nm.

	Corrected calibration curve slope	$\frac{Slope_{fibre}}{Slope_{cuvette}}$	Theoretical power factor	% Difference
Fibre 1	0.0008	2.1 x 10^{-3}	1.8 x 10^{-3}	-15
Fibre 2	0.0028	7.3 x 10^{-3}	8 x 10^{-3}	-9

Following the validation of the fibre measurements with the cuvette measurements, the next step in the experiments was to use test the in fibre platform using real wine. This experiment was done using fibre 2 (Figure 6B) and white wines number 6 and 7. Four separate vials of the mixed PRA working solution and wine were used to make four absorbance measurements for each wine. In these experiments the PRA concentration was $7.8x10^{-4}$ mol/L and no filtering was used as in these first experiments the experimental method had not yet been fully refined. However, these results are still valid as the absorbance is not dependent on PRA working solution concentration given that the concentration is high enough (see Figure 9). The free sulfite concentration in these wines was determined using the aspiration method on the same day. The room temperature where the fibre measurements took place was about 19°C while the room temperature where the wines were aspirated was about 23°C.

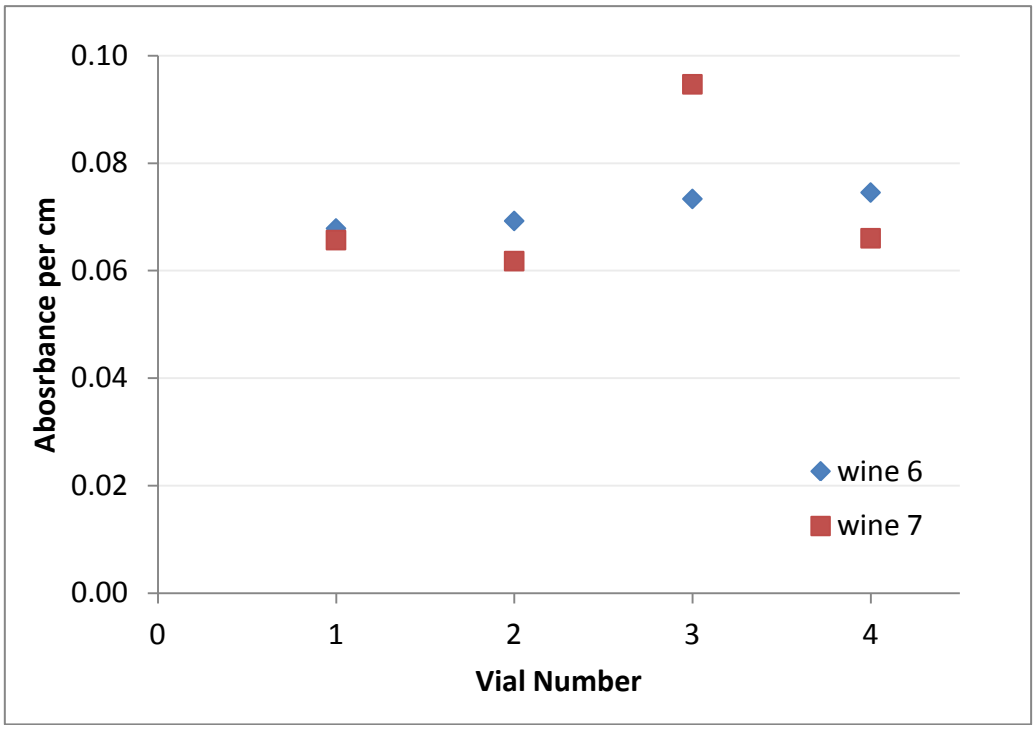


Figure 22: Absorbance per cm of real wine samples mixed with $7.8x10^{-4}$ mol/L PRA working solution.

The absorbances are quite consistent for both wines, except for vial 3 in wine 7 due to particulates filling into the fibre (which was observed under the microscope after the measurement). The coefficient of variation (CV) for wine 6 is 4.5% while the CV for wine 7 excluding vial 3 is 3.7%.

Using the equations of the in-fibre calibration curve (Figure 21), the sulfite concentrations in the wine samples were calculated and compared to the sulfite concentration from the aspiration method (Table

3). These values are lower than both the aspiration method and the cuvette measurements, but still show that wine 7 had a lower sulfite concentration when compared to wine 6. This discrepancy can be attributed to the different temperatures the fibre and aspiration measurements were taken. As shown in cuvette (Figure 16), the sulfite concentration increases with temperature (about 1 ppm per degree) which is in agreement with the difference. These results are very promising as the in fibre measurements agree with the standard method, and the wine has had minimal processing and thus has the potential to be implemented into the 'smart bung' device.

Table 3: In-fibre absorbance values and corresponding concentration of SO_2 in white wine samples and actual SO_2 concentration from the aspiration method.

sample	absorbance per cm	Sulfite concentration (ppm)	Aspiration method (ppm)
Wine 6, vial 1	0.06786	22.8	
Wine 6, vial 2	0.06926	23.8	
Wine 6, vial 3	0.07336	26.7	
Wine 6, vial 4	0.07455	27.5	
average	0.07126	25.2	29
Wine 7, vial 1	0.06570	21.2	
Wine 7, vial 2	0.06179	18.4	
Wine 7, vial 3	0.09469	41.9	
Wine 7, vial 4	0.06604	21.5	
average (excluding vial 3)	0.06451	20.4	26

The experiment was repeated again, with filtering of the coloured solution prior to loading the liquid into the fibre. The aspiration method was performed with temperature control so that the solution was consistent with the room temperature where the fibre measurements took place. In these experiments, wines 1 and 2 were used, which had been treated with hydrogen peroxide to bring the free SO_2 concentration to about 10 ppm – the lower range of detection. The sulfur dioxide concentration in the samples was calculated using the calibration curve (Figure 21) and the results are summarised in Table 4. The fibre measurements of wine 1 agree well with the concentration determined by the aspiration method (on average, 10% lower). However, the absorbance measurements for wine 2 were much higher than expected – around 30 ppm when it should be 11 ppm.

Table 4: In-fibre absorbance values and corresponding sulfite concentration using wine samples 1 and 2 and actual sulfite concentration from the aspiration method.

	Absorbance per cm	Sulfite concentration (ppm)	Aspiration method (ppm)
Wine 1, vial 1	0.05321	12.3	
Wine 1, vial 2	0.05237	11.7	
Wine 1, vial 3	0.04634	7.4	
Wine 1, vial 4	0.04081	3.4	
Average	0.04818	8.7	10
Wine 2, vial 1	0.07552	28.2	
Wine 2, vial 2	0.07853	30.4	
Wine 2, vial 3	0.07867	30.5	
Wine 2, vial 4	0.08902	37.9	
average	0.08044	31.7	11

This discrepancy may be due to several factors. Firstly, the fibre measurements assume that any change in absorption is due to different free sulfite concentration. However, there may be other absorption mechanisms due to the fibre set up that is unrelated to the sulfur dioxide present in the sample (that may or may not be seen in the bulk cuvette experiments). We have designed a more complex experimental setup to enable any other absorbances to be separated from the absorbance due to sulfte concentration (see Figure 23). Instead of looking at the absorbance at one wavelength only, a second laser is simultaneously introduced into the sample. The wavelength of this laser is chosen such that there is no expected absorbance from the sample (about 660 nm and higher, based on Figure 8). This second laser can be used to calibrate the first reading, as any absorbance at this wavelength would not be due to the sulfites in solution. Given the limited time available in this project, only preliminary testing was completed with the alternative set up in Figure 23.

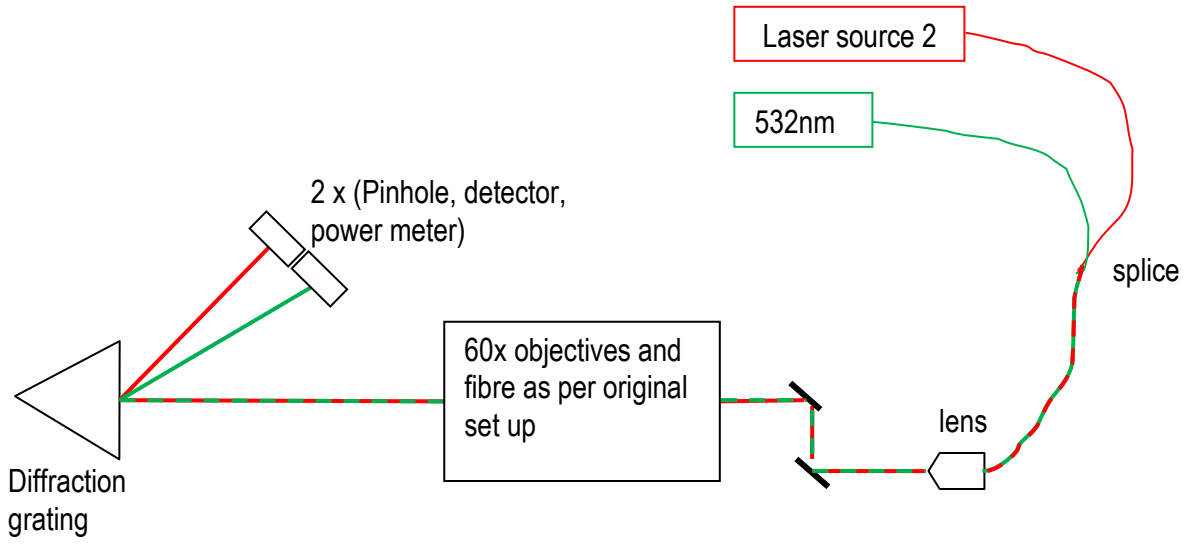


Figure 23: Alternative set up to remove any absorbances from the fibre from the absorbance due to the presence of sulfites in the sample. The two lasers are fibre coupled into the lens and the diffraction grating splits the two light sources to separate detectors.

6.3 Other related progress

During the period over which this work was performed, other research within IPAS demonstrated the proof of concept of surface-functionalised chemical sensors based on suspended-core optical fibres. In particular, surface functionalised fibres have been successfully used for aluminium sensing [16] and hydrogen peroxide sensing [unpublished work]. This work was funded by Tanya Monro's Federation Fellowship program. Note that this work enables sensing within <10 nL sample volumes for the first time. While surface-functionalised sensors were not explored for measuring SO_2 within this work we have proposed previously that such new technologies should also be explored as possible "smart bung" components.

In addition, work funded by Tanya Monro's Federation Fellowship program within the period of this project has also enable the detection of fluorophores at concentrations of < 10 pM; this represents more than an order of magnitude improvement in sensitivity over the course of this project [17].

7 Outcomes and Conclusions

We have shown that model wine sulfite solutions can be quantified using the pararosaniline reaction in bulk liquid samples and that equivalent results can be obtained in microstructured optic fibres (MOF). We have also demonstrated that sulfites can be detected and quantified in white wine samples and have identified a route to optimising this technique in subsequent work. This was the major goal of the GWRDC funded pilot study.

The results of this project show that the use of MOF for the measurement of sulfites in wine is a possible solution to achieving constant, near real time wine monitoring cheaply and autonomously. Further work on validations is needed as highlighted where appropriate throughout this report. The flexibility of the MOF platform, such that its optical properties can be specifically tailored to maximise the interaction of the sample with the light means that that detection of sulfites is simplified as samples do not require dilution for analysis. It is the simplicity of this technique which would allow it to be utilised on a large scale and allow winemakers to ensure the quality of their wines throughout the wine making process.

This project has achieved its aims and made progress towards demonstrating a proof of concept device for the monitoring of free SO_2 in wine. To achieve this we have utlitised a chemical reaction that is known and extensively documented and adapted it to a completely new platform. The use of microstructured optical fibres (MOF) promises to provide the low cost, real time monitoring solution that the industry desperately craves.

8 Recommendations

We have demonstrated the basic approach to the detection of sulfites using MOF's. In order build on this work and to develop it into a prototype for the 'smart bung' process more work will have to be performed in the following areas.

- Wine Analysis

  In-depth analysis of different types of wine to investigate the reaction between the wine and the sensing compound in order to determine whether the increase in absorbance over time is constant for all wines and whether there are other compounds that may interfere with the analysis. The successful analysis of several white wines within this project appear to indicate that is not likely to be a significant problem.

- Fibre core size and level of detection

  Investigate the effects of different types of MOFs and determine the lowest/highest detectable threshold for sulfites in wine. The interaction of the sample with the light can be altered in several ways. The core size can be increased to allow for less light to interact with the sample, or it can be decreased to that more light emerges into the "holey" region. The length of the fibre also has an effect as longer fibres allow for more interaction between the light and the sample than with a short length of fibre.

- Fibre material

  The work thus far has been based on a lead silicate (F2) glass optical fibre. However, ultimately, the smart bung is likely to perform better if made from a silica glass optical fibre, since silica glass fibres are more robust and have lower intrinsic absorption. During the period of this GWRDC project, IPAS successfully commissioned a silica optical fibre fabrication facility. While at present it is not yet possible to fabricate fibres of the type required for the smart bung work using this facility (namely the "suspended-core" fibre type) this is a short-mid term goal, and such fibres will be available to further smart bung development projects in the future.

– Fibre based sensing platform

As stated, the easiest way to detect and sense directly from the barrel would be with a dip-sensor. With this type of sensor, the analyte is surface functionalised and attached to the surface of the holes and hence when the wine reacts with the surface coating, the detectible change can occur in-situ. Light can be shone into the core and detected at the same end by detection and quantification of power in the backscatter. The other, slightly easier, approach would require the analyte and the wine to first be mixed prior to drawing it into the fibre for measurement. One such way that this can occur is with a micro-mixing 'T', which allows nano-litre volumes of sample to enter a T-junction via two ports, mix, and then be drawn out through the third junction. The other possibility for premixing can occur using a mixing chip. This chip is essentially a piece of glass which has a path etched out. Small ports allow for the wine and analyte to be introduced into the path and as the analyte and the wine fill the path, they are merged together where they can mix. During this project, initial feasibility work on the use of such mixing T's was performed, and we demonstrated that it is possible to integrate our microstructured optical fibres with these devices, and that the fibres can be loaded with fluids using these devices.

– Prototype

Produce a demonstration of a working sensor system that would allow the sample to be mixed and the fibre to be filled with the mixed sample, and the detection and quantification of the sulfur dioxide to be performed.

The fulfilment of this final point represents the successful development of a prototype of a "smart bung".

In addition to free sulfur dioxide, there are 5 others parameters that are considered to be important in wine making which still need to be investigated. Once this is achieved the 'smart bung' sensing platform will become a reality for incorporation within wineries.

9 Appendices

9.1: Communication

9.1:1 Progress report for Smart bungs GWRDC grant

Progress Report: Smart Bungs, GWRDC Grant UA 1003

Report Prepared: 19/10/10

The project, titled "**Smart Bungs**", which commenced in July 2010, has already shown considerable progress. After consultation with the GWRDC, an initial three-year grant application was pared back to one-year and was to be a 'pilot study' concerning the *in-situ* measurement of sulfur dioxide (SO_2). After reviewing the options available to tackle this task, and the substantially reduced budget available, it was decided that a microfluidics-based approach would be taken (please see further details below).

The work within the current (10/11) GWRDC Smart Bungs project has 2 components: A) work on the demonstration of a fluorophore suitable for use with wine samples, and B) work on the microfluidic mixing system and subsequent optical fibre based measurement. Significant progress has been made in both areas, as described briefly below.

A. Fluorophore selection & testing

Katarina Markulic (Chemist with a BSc (Hons) degree) was hired in June 2010 to perform this research work. The aim of this work, using commercially available fluorophores identified in the literature as exhibiting a SO_2 – dependent change in fluorescence, was to test the capacity of these fluorophores for 1) their function in model wine solutions, 2) providing a means of quantifying the SO_2 concentration in model wine and 3) their suitability for use within the fibres.

We have been able to show that a selected fluorophore (Rhodamine6G, R6G, identified from the literature) undergoes fluorescence in both methanol and some model wine solutions. While we have observed a linear relationship between the concentration of R6G and fluorescence intensity in both media, this relationship was not so straightforward when tested against SO_2. It was felt that the presence of certain components of the model wine, might be quenching the R6G. It is now felt that R6G

might not be the most suitable fluorophore and others are being investigated. One particular such fluorophore (pararosaniline, PRA) appears very promising.

B. Microfluidics development

In this approach, the microstructured fibre itself serves as a platform for the interaction between the light and the wine sample that fills its holes, with the mixing of the wine sample and the fluorophore solution (required to produce to quantifiable change in response to the sulfur dioxide level) occurring "off-fibre" within a microfluidic mixing chip. Note that ultimately, it would be attractive to use surface functionalised fibres that provide a direct fluorescence response when inserted in the Smart Bung. However, this was not feasible given the reduction to both the time and the level of funding provided. For the current system under development, the Smart Bung concept still holds true, although in a modified form in which a fine capillary sits within the bung, extracting a small fluid volume, that is then mixed with a fluorophore solution via a microfluidics system, and loaded into the fibre, where the detection is performed.To reduce risk, two distinct approaches to the microfluidics mixing are being evaluated within this project. The first (see **Figure 1**) uses a microfluidic-mixing chip (sourced via collaboration with the NCRIS-funded microfluidics facility at the Wark Institute at UniSA) and the second (see **Figure 2**) uses a commercially sourced "T" junction for mixing the fluid samples.

Figure 1 shows an early prototype of the microfluidic chip approach (the etched lines on the glass slide). In this approach, the wine sample and fluorophore solution are introduced to the chip via the red ports, and the fibre can be filled by inserting it on one of the red ports at the other end of the chip. However, while some progress has been made with this approach, and because the facility at UniSA is only newly established with relatively high turnaround times, there is not as yet much experience in creating solutions that are compatible with fibres. Thus, this is viewed as the higher risk approach of the two under consideration. However, it is being pursued because this approach ultimately offers high flexibility for working with multiple fluorophores and sensing fibres.

Figure 2 shows the simpler "T" mixing system. Using this approach, the wine sample and the fluorophore are introduced into the T via the side capillary ports, and the sensing fibre collects the sample from the central arm of the T (to the right in Figure 2). Progress has been made with this approach – we have shown that we can fill the fluid samples from the input capillaries, through the relatively small volume (approx 50 nL) of the T device itself, and load the detection arm of the system. The next experiments planned for this configuration include the use of a microstructured fibre on the

detection arm to confirm the efficacy of the mixing achieved. Once this is fully characterised, this system will be suitable for testing the fluorophores emerging from part A.

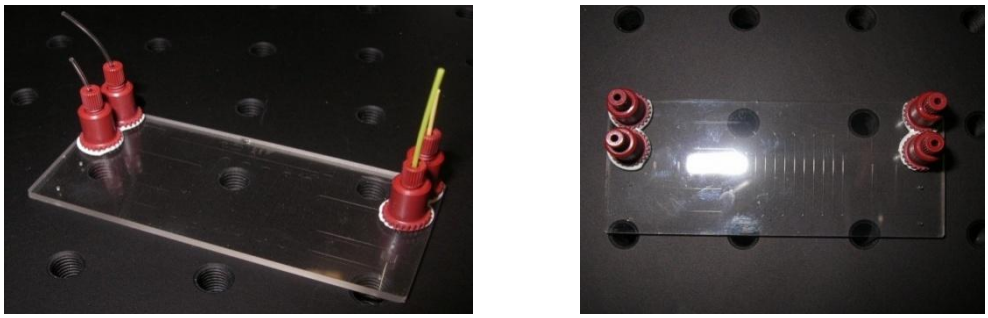


Figure 1: Microfluidic chip approach - first prototype mixing chip.

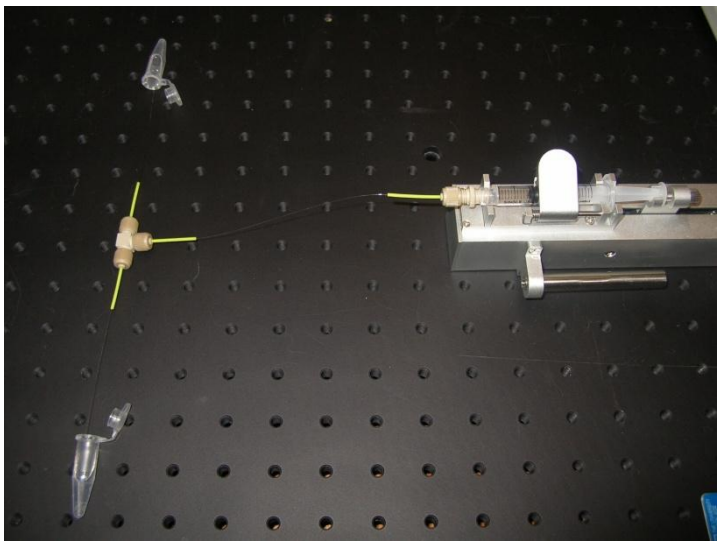


Figure 2: The second microfluidic mixing approach – the "T" mixing sytem.

Other related progress

An alternative approach to the microfluidic mixing approach described above involves immobilising the fluorophore on a solid support (note that this is conceptually similar to the approach proposed in the original GWRDC application, and subsequently dismissed due to lack of resources). Initial investigations into this approach required the doping of PDMS polymer tubing with fluorophore, again R6G. The doped polymer tubing showed a good signal, which was considerably attenuated when the doped polymer was exposed to a sulfur dioxide solution (see **Figure 3**). Further work is needed to determine whether this approach can accurately quantify the sulfur dioxide concentration, and how best to integrate this immobilization technique with the fibre sensing platform.

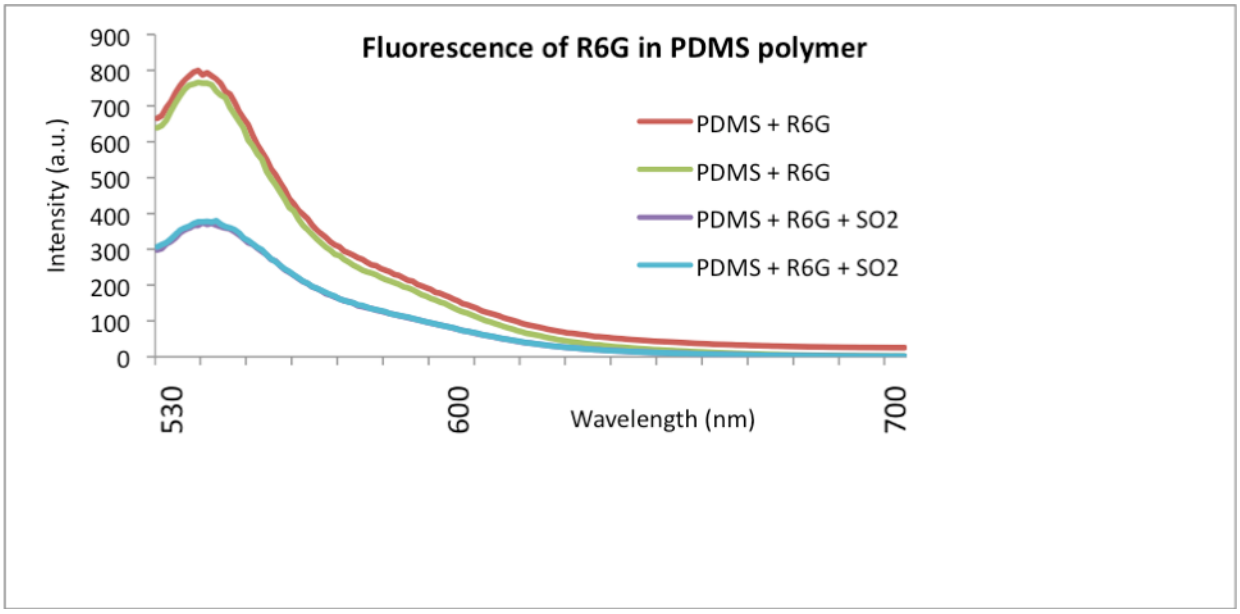


Figure 3: Change in fluorescence from a bulk sample of polymer doped with Rhodamine 6B in the presence of sulfur dioxide.

In addition, during the duration of this project, progress has been made in fabricating microstructured fibres with larger, "inflated", internal holes, which has allowed the more rapid fluid filling of these fibres. This will enhance the practicality of the Smart Bung sensing approach by reducing the time between measurements.

Overview of project progress to date

Based on the originally listed Outputs and Achievements form the grant proposal (**Table 1**) it can be seen that we are on or ahead of schedule with the major milestones of the project. The proposed outputs and activities for the continuation of the grant can be found in **Table 2.**

In summary, the project has only been underway for some three months but has shown considerable early progress. We expect the microfluidic aspect of the project to be more successful under the action of the new PRA fluorophore, while the surface immobilisation technique also appears highly promising. However, to bring these various threads together into a demonstration of sulfur dioxide sensing requires a 2nd year of GWRDC funding.

Table 1: Outputs and Activities as listed in original GWRDC Proposal.

Year 1	Output	Target Date mm/yy	Status	Activities
A	Team capable of developing optical fibre based SO_2 sensors	07/10	Completed	Hire qualified, dedicated team Establish regular team meetings Dedicate laboratory space to project activities
B	Consumables & sensor development fibres	09/10	Ongoing Completed	Dedicated optical fibre fabricated for testing purposes Purchase commercial fluorophores suitable for quenching with SO_2
C	Optical detection of SO_2 fluorophore quenching of commercial fluorophores in solution	12/10	Completed Ongoing	Construct a laboratory-based experimental test-bed for evaluating the sensor performance Determine fluorescence changes when SO_2 is mixed in solution with commercial fluorophores & demonstrate linear dependence on SO_2 concentration
D	Optical detection of SO_2 quenching of fluorophores within the optical fibres	03/11	Ongoing	Demonstrate efficacy of in-fibre sensing, including preliminary evaluation of the microfluidic mixing system using test solutions
E	Proof of concept optical fibre based SO_2 sensor	06/11	Ongoing To be done To be done	Perform laboratory based characterisation of the performance of the sulfur dioxide-based dip sensor based on model wines Compare results with those from standard measurement techniques Test feasibility on (real) wine samples

Table 2: Outputs and Activities for proposed extension of Smart Bungs grant

Year 2	Output	Target Date mm/yy	Activities
A	Demonstration of linear performance of selected fluorophore to sulfur dioxide in model wine within a fibre	Dec 2011	Calibration of solutions using traditional chemical means in all relevant media (methanol, model wine, commercial wine) at varying pH levels. Measurement of these calibrated solutions using the optical sensor
B	Demonstration of the operation of the microfluidics-based mixing system	September 2011	Calibration of microfluidics system, demonstration of effective and reproducible mixing of fluorophore solutions with sample solutions
C	Demonstration of the microfluidics based mixing system integrated with the optical fibre detection platform	Dec 2011 February 2012	Demonstration of techniques for loading the sensing fibre. Demonstration of calibration and alignment techniques for the proof of concept sensor in control solutions, including model wine.
D	Demonstration of the potential of immobilized fluorophore approach	April 2012	Demonstration of concentration dependence of the immobilized fluorophores, and assessment of pathways to integrating the immobilization approach with the fibre sensing platform.
E	Prototype fibre-based sulfur dioxide sensor Plan for future development of smart bungs	June 2012 June 2012	Laboratory-based demonstration of complete sensor prototype on model wine solutions. Report on future development opportunities for the smart bung approach.

9.1.2 :R&D at Work Article [18]

GWRDC
GRAPE AND WINE RESEARCH AND DEVELOPMENT CORPORATION

R&D AT WORK

APRIL 2011

Optical fibres give hope of big savings

It will be quality up and wastage down if the promise shown in early stages of exciting new wine sensor research involving optical fibres is fulfilled.

Development of the technology, dubbed "a smart bung", is a classic case of a good idea coming from cross-disciplinary discussion among scientists. It is also a demonstration of how industry can visualise an outcome and put the scientists to work to find a way of achieving it. Inspiration came from a presentation on optical fibres by Professor Tanya Monro, Director of the University of Adelaide's Institute for Photonics & Advanced Sensing (IPAS). The university's Professor of Oenology, Dennis Taylor, whose specialist area is wine chemistry, discussed potential use in the wine industry with her as well as with fellow wine researchers.

Today, team members (who include Tanya Monro, Dennis Taylor, Heike Ebendorff-Heidepriem, Rachel Moore, Mai-chi Nguyen, Gordon Elsey and George Skouroumounis) are working towards devising a simple means of sensing the presence and levels of certain compounds in wine. These researchers bring experience spanning physics, chemistry and wine sensory research.

The "smart bung" term helps us imagine how the technology would work - optical fibres, which are cheap, embedded in every stopper of every barrel, send off messages about what is happening. The optical fibre sensors can detect chemicals or biomolecules in very small amounts of wine and opens up the prospect of regular monitoring

Progress is monitored and warning signals are given immediately something unwanted occurs from a remote position and without needing to move barrels. There is also no need to pull out the bung with its associated risks of oxygen ingress and contamination.

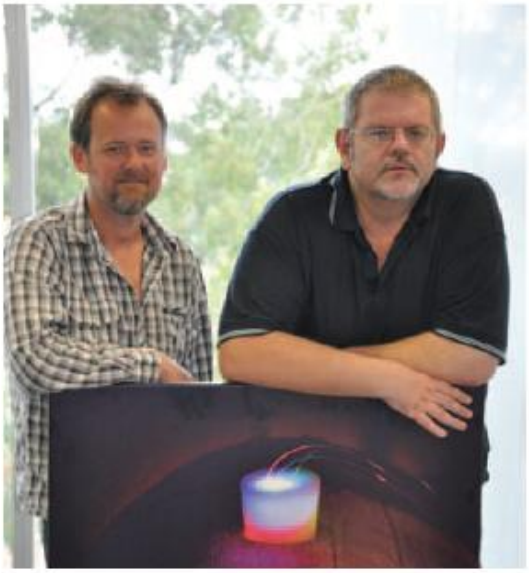
Funding from the Grape and Wine Research and Development Corporation (GWRDC) and the University of Adelaide is enabling a pilot project to be conducted with a focus on free sulfur dioxide.

"It has been shown that the technology works for this compound, opening up the prospect for the principle to be applied to othercomponents," Dennis Taylor said. "An industry reference group has been very encouraged and has listed 14 parameters, ranging from ethanol content to potential taints, which are likely to be the subject of expanded work down the track."

Initial results suggest there is the possibility of applying the technology throughout the production chain from grape transport to the bottle, although most interest will be at the critical points of fermentation and maturation.

Makers of other beverages such as fruit juices and beer will also be interested in this Australian innovation. This is an early stage, however, and considerable work needs to be done before refinement of a prototype and eventual commercialisation.

Project team member Dr Gordon Elsey sees significant advantages on two main fronts. The first is winemaking practice, with labour savings, the peace of mind of an alert, real-time quality control system, and the convenience of a remote system of recording and assembling information. "The second boost will be to the economy of winemaking," he said. "With sensors at all points winemakers will know whether a problem (e.g. presence of Brettanomyces) is confined to a small number of barrels, for instance, or is more widespread. This will avoid wastage and ensure one part of the batch does not contaminate the lot when it comes to bottling. "There is also the potential saving through being alerted to the development of a problem and being able to correct it or isolate it. In that sense we see this as an 'early warning system' for wine quality which would allow for prompt remedial measures to be undertaken."



Research team members Dennis Taylor, left and Gordon Elsey see "smart bung" technology having the potential to boost winemaking efficiency.

9.1.3: Advertiser article [19]

Wine to thrill the sensors

By CLARE PEDDIE

From: *The Advertiser*
October 22, 2009



VINTAGE IDEA: PhD student Shaghik Atakaramians with the ``smart bung'' whose optical fibres test the wine.
Picture: BRENTON EDWARDS

TINY optical probes are being developed as an "early warning system" for winemakers who want to check wine maturity without opening the barrel.

The technology, being developed at the University of Adelaide, will allow them to monitor and fix problems as they arise, without interfering with wine that should have been left in the barrel.

Professor Dennis Taylor, from the School of Agriculture, Food and Wine, is working on a prototype with Professor Tanya Monro at the Institute for Photonics and Advanced Sensing.

"It's a long-term project but it's a brand new one, a leap forward," Professor Taylor said.

"No one has ever done this sort of thing before, or thought about doing this sort of thing before."

Instead of pulling out the stopper and sampling every barrel, the winemaker will be able to monitor the temperature and chemical composition from afar.

Optical fibres in the "smart bung" transmit light of specific wavelengths into the barrel.

The light interacts with the wine and results are relayed to a computer.

"It would revolutionise the industry because they all rely on these old, boring time-consuming tests," Professor Taylor said.

"We would have an early warning system that could be used not only for wine but all sorts of things like beer and everything else."

PhD student Shaghik Atakaramians said tiny sensors could be used "to solve lots of problems".

"We can put the tiny fibres in an environment where people cannot reach, where it is toxic or where you cannot easily do experiments," she said.

"Using these sensors and inserting them in that environment is, in my opinion, really interesting and it drives me."

9.1.4: Poster presented at the Nanophotonics Workshop [20]

INSTITUTE FOR PHOTONICS & ADVANCED SENSING

FREE SULFUR DIOXIDE SENSING IN WINE

THE UNIVERSITY of ADELAIDE

Mai-Chi Nguyen[1], Rachel Moore[1], George Skouroumounis[2], Dennis Taylor[2], Heike Ebendorff-Heidepriem[1], Tanya Monro[1]

[1]Institute for Photonics and Advanced Sensing, School of Chemistry & Physics, The University of Adelaide

[2]School of Agriculture, Food & Wine, The University of Adelaide

PROJECT OBJECTIVES

- Develop an optical fibre sensor using microstructured optical fibre (MOF) to detect free sulfur dioxide in wine in a rapid, non intrusive manner
- Characterise the performance of the sensor on model wines
- Test technique on real wine samples and compare to standard techniques

BACKGROUND

Sulfur dioxide (SO_2) is an antimicrobial and antioxidant additive.

- Free sulfur dioxide (SO_2, SO_3^{2-} & HSO_3^-) provides these effects
- White wine with <10ppm free SO_2 have a substantial oxidised aroma [1]
- Aim to have ~30ppm free SO_2 in wine

The Australian wine industry standard test for free SO_2 is the aspiration method [2].

- Exposes the remaining wine in the barrel to air — chance of spoilage
- Requires sample volume ~20mL
- 15 minute reaction time

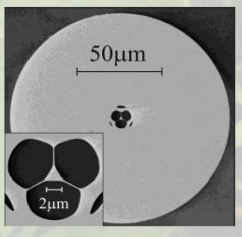
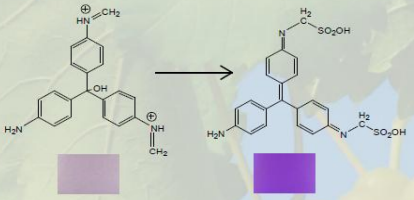


Figure 1: Scanning Electron Microscope (SEM) image of the fibre used in the experiments.

MOFs have been used as evanescent absorption sensors [3], where the analyte in the holes (Fig. 1) interact with the guided light.

SENSOR CHARACTERISATION

The colourimetric reaction between pararosaniline hydrochloride (PRA), formaldehyde and SO_2 was selected [4], [5].



- Performance characterised using model wine in cuvette and in fibre (Fig. 2)

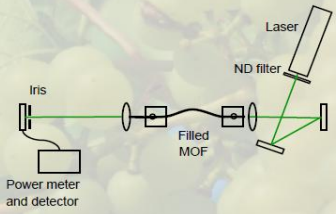


Figure 2: Experimental set up for the in-fibre measurements

- The linear range can be altered via changing the PRA concentration (Fig. 3)

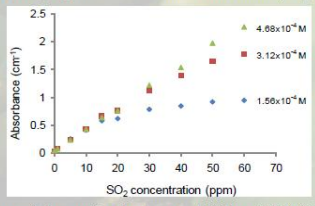


Figure 3: In-cuvette absorbance at 532nm of PRA-SO_2 in model wine solution for different PRA concentrations.

- Cuvette (Fig. 3) and fibre measurements (Fig. 4) agree

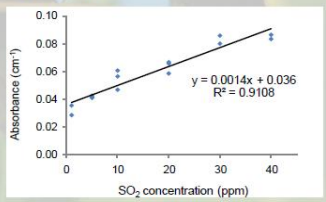


Figure 4: In-fibre absorbance at 532nm of PRA-SO_2 in model wine solution

This project was funded by the Grape and Wine Research and Development Corporation (GWRDC).

SENSING IN REAL WINE

Three white wines were tested for SO_2 in cuvette and compared to the aspiration method.

- Absorbance in wine continues to increase with time
- The calculated SO_2 concentration in the wine agrees with the standard method after 3 minutes (Fig. 5)

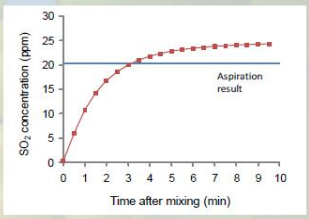


Figure 5: Absorbance of the real wine with PRA vs time at 532nm (cuvette measurements).

- Fibre experimental set up in Figure 2 doesn't work with real wine—need a more sophisticated technique

FUTURE WORK

- Devise and characterise a fibre sensor technique that works on real wine
- Develop microfluidic mixing system to integrate with the detection platform
- Expand sensing technique to monitor other quality indicators in wine

REFERENCES

[1] P. Godden *et al.*, Aust. J. Grape Wine Res., **7**, 64–105 (2001).

[2] B. Rankine and K. Pocock, Aust. Wine Brew. Spirit Rev., **88**(8), 40, 42, 44 (1970).

[3] X. Yu *et al.*, Sens. Actuators, B, **137**, 462-466 (2009).

[4] P. West and G. Gaeke, Anal. Chem., **28**, 1816-1819 (1956).

[5] L. Gibson *et al.*, Anal. Chim. Acta, **623**,109-116 (2008).

9.2: Intellectual Property

This project is underpinned by three background patents all owned by the University of Adelaide, which have all been granted in certain jurisdictions with others pending:

1. Method and Device for forming micro-structured fibre.
2. Optical Fibre Sensor.
3. Fabrication of Nanowires.

These technology platform patents cover the methods of producing soft glass microstructured fibres, suspended core fibres, exposed core fibres and underpin many IPAS sensing projects in areas from Wine Production to Reproductive Health.

The University of Adelaide, utilising the services of its commercial company Adelaide Research & Innovation Pty Ltd, constantly develops intellectual property (IP) to generate commercial value. The aim is to make the IP available for the mutual benefit of university staff and Australia generally. Opportunities are evaluated by consultation with potential partners (public and/or private sectors) and understanding the market to optimise the most appropriate path to market for IP. Hence the benefits and commercial risks are shared with partners engaged to participate in the development of opportunities from the university. Our approach therefore is to manage IP in parallel with a commercial strategy.

The intellectual property developed within this project includes but is not limited to:

Knowledge pertaining to the affinity between fluorophore sensors and SO_2;

Performance of the fluorophore(s) in the presence of wine (including pH effects, etc);

Advances in the development of integrated microfluidics-fibre sensing devices;

Advances in fibre-optic technology for sensing sulfur dioxide in wine;

9.3: References

1 Rankine, B. *Making good wine: a manual of winemaking practice for Australia and New Zealand*. Sun: 1991, 106-110.

2 Sharma, A., Wolfbeis, O. The quenching of the fluorescence of polycyclic aromatic hydrocarbons and Rhodamine 6G by sulfur dioxide. *Spectrochimica Acta.* **1987,***43* (11),1417-1421.

3 Schiff, H. Eine neue Reihe organischen Diaminen. Justus Liebigs Ann Chemie.**1866**, *140*, 92-137.

4 Robins, J., Abrams, G., Pincock, J. The structure of Schiff reagent aldehyde adducts and the mechanism of the Schiff reaction as determined by nuclear magnetic resonance spectroscopy. *Can. J. Chem./Rev. can. chim*. **1980**, 58(4): 339-347.

5 West, P., Gaeke, G. Fixation of sulfur dioxide as disulfitomercurate (II) and subsequent colorimetric estimation. *Anal. Chem.* **1956**, 28, 12, 1816-1819.

6 Official Methods of Analysis, 16th ed.; AOAC International, Gaithersburg, MD, 1995; Method 693.11.

7 Official Methods of Analysis, 16th ed.; AOAC International, Gaithersburg, MD, 1995; Method 963.20.

8 Gibson, L., Kerr, W., Nordon, A., Robertson, C., Turnbull, L., Watt, C., Cheung, A., Johnstone, W. On-site determination of formaldehyde: A low cost measurement device for museum environments. *Anal Chim Acta.* **2008**, 623, 109-116.

9 Segundo, M., Rangel, A. A gas diffusion sequential injection system for the determination of sulfur dioxide in wines. *Anal. Chim. Acta.* **2001**, *427*, 279-286.

10 Ebendorff-Heidepriem, Heike; Warren-Smith, Stephen; Monro, Tanya Mary. Suspended nanowires: fabrication, design and characterization of fibers with nanoscale cores. *Opt. Express.* **2009**, 17(4), 2646-2657.

11 Nauman, P., West, P., Tron, F., Gaeke, G. A spectrophotometric study of the Schiff reaction as applied to the quantitative determination of SO_2. *Anal Chem*. **1960**, *320*, 1307.

12 Hormann, H., Grassmann, W., Fires, G. Über den mechanismus der Schiffschen reaction. *Justus Liebigs Ann Chemie*. **1958,***616*, 125-147.

13 Pate, J., Lodge, J., Wartburg, A. Effect of pararosanaline in the trace determination of sulfur dioxide, *Anal. Chem.***1962**, 34,12, 1660-1662.

14 Huitt, H.; Lodge, J., Equilibrium effects in determination of sulfur dioxide with pararosanaline and *formaldehyde.* *Anal. Chem.* **1964**, *36*, 1305-1308.

15 Rankine, B. C., Pocock, K. F. Alkalimetric determination of sulphur dioxide in wine. *Aust. Wine Brew. Spirit Rev.* **1970**, *88*, 40-44.

16 Warren-Smith, S., Heng,S., Ebendorff-Heidepriem, H.,Abell, A., Monro, T. Fluorescence-Based Aluminum Ion Sensing Using a Surface-Functionalized Microstructured Optical Fiber, Langmuir. **2011**, *27*, 5680–5685.

17 Schartner, E., Ebendorff-Heidepriem, H., Warren-Smith, S., White, R.,Monro, T., Driving down the Detection Limit in Microstructured Fiber‐Based Chemical Dip Sensors, *Sensors* **2011**, *11*, 2961-2971

18 Optical fibres give hope of big savings,*R&D@Work*, April 2011, p.1.

19 Peddie, C. Wine to thrill the sensors, *The Advertiser*, October 22, 2009.

20 Nguyen, M., Moore, R., Skouroumounis, G., Taylor, D., Ebendorff-Heidepriem, H., Monro, T. Free Sulfur Dioxide Sensing in Wine. Poster session presented at: Nanophotonics for sensing & nonlinear optics Workshop: Next generation photonic materials, structures & devices; 24-26th August 2011; McLaren Vale, South Australia.

9.4: Staff

Rachel Moore: Research Officer at The University of Adelaide
BSc (Hons) Organic Chemistry, BTech (forensic and analytical chemistry)
Role: perform research into possible analytes for the detection of SO_2 (sulfites) in solution
Perform bulk scale testing in order to optimise the technique.

Mai-Chi Nguyen: Research officer at The University of Adelaide
BSc (Physics), BEng (Hons) (Mech & Aero)
Role: optimise the micro-fluidics set up to perform detection and quantification of SO_2 in microstructured optic fibres (MOF's).

George Skouroumounis: Principal Research Chemist at The University of Adelaide
Phd, Bsc(Hons), Grad. Dip. Oenology.
Role: advice on SO_2 measurements.

Heike Ebendorff-Heidepriem: Deputy Director of the Centre of Expertise in Photonics Institute of Photonics and Advanced Sensing School of Chemistry & Physics at The University of Adelaide

Gordon Elsey
Phd, Bsc(Hons).
Role: assisted grant writing.

Dennis Taylor: Chair and Professor of Oenology, Adjunct Professor of Organic Chemistry at The University of Adelaide
Role: Oversee project team.

Tanya Monro: Director, The Institute for Photonics & Advanced Sensing (IPAS) at The University of Adelaide. Director, Centre of Expertise in Photonics (CoEP). ARC Federation Fellow, FTSE, FAIP
Role: Oversee project team.

9.5: Additional Data

Table 5: Absorbance values for sulfite solutions containing 10% ethanol in both water and saturated KHT solution

		Development Time (Minutes)								
		0	1	2	3	4	5	6	7	8
Absorbance EtOH in water	1 PPM Sulfites	0.374866	0.57111	0.654345	0.691346	0.707051	0.71276	0.714183		
	5 PPM Sulfites	0.540377	1.604598	2.162683	2.454846	2.618535	2.718644	2.769675	2.800117	2.814208
	10PPM Sulfites	0.74184	2.280284	3.099532	3.565207	3.857536	4.045635	4.179029	4.262077	4.34376
Absorbance EtOH in Sat. KHT	1 PPM Sulfites	0.193434	0.513393	0.675367	0.754075	0.792275	0.81211	0.821394		
	5 PPM Sulfites	0.536165	1.604815	2.191232	2.522894	2.727972	2.852863	2.940295	2.994854	3.026412
	10PPM Sulfites	0.776046	2.339902	3.134633	3.614803	3.897174	4.103322	4.244491	4.323352	4.405946

Note: this is the raw data for the information presented in Figure8.

Table 6: Absorbance results for coloured solutions containing different concentrations of PRA

PRA conc (mol/L)	Sulfite equivalent (1:1 ratio)	Sulfite Concentration									
		0	1	5	10	15	20	30	40	50	60
1.56×10^{-4}	10ppm equiv.	0.046165	0.094914	0.312525	0.514552	0.733938	0.789281	1.019623	1.11606	1.236774	1.28481
3.12×10^{-5}	20ppm equiv.	0.033429	0.091619	0.306591	0.56515	0.877385	1.013214	1.513875	1.885566	2.270111	2.457553
4.68×10^{-6}	30ppm equiv.	0.046544	0.090465	0.310155	0.572116	0.864655	1.029876	1.670768	2.123688	2.740356	3.145552

Note: This is the raw data for the information presented in Figure 9.

Table 7:Absorbance values for sulfite solutions at varying wavelengths.

Wavelength		Sulfite Concentration (PPM)										
		0	1	5	10	15	20	25	30	40	50	60
Absorbance values at different wavelengths	Max	0.045673	0.112292	0.371763	0.674361	0.971179	1.310239	1.561902	1.915483	2.329743	2.836107	3.258136
	550	0.042205	0.107125	0.360502	0.654196	0.942958	1.27228	1.516517	1.857942	2.256706	2.738455	3.13235
	540	0.037119	0.093865	0.313438	0.568228	0.818355	1.101876	1.311934	1.60285	1.944335	2.354111	2.696719
	532	0.031806	0.079375	0.263781	0.478285	0.69001	0.930201	1.108545	1.355586	1.650544	2.007775	2.314082
	530	0.031343	0.076678	0.252758	0.458115	0.660294	0.890459	1.061684	1.299536	1.583428	1.930292	2.230007

Note: This is the raw data for the information presented in Figure 12. Note that these values were used to determine the calibration curve in Figure 13.

Table 8: Maximum absorbance values for sulfite solutions containing 10% and 20% ethanol

Ethanol percentage	Sulfite Concentration (PPM)					
	0	5	10	20	40	60
Maximum absorbance with 10%	0.049234	0.382439	0.714821	1.32819	2.346908	3.280334
Maximum absorbance with 20%	0.051473	0.355038	0.682778	1.309691	2.419435	3.309767

Note: This is the raw data for the information presented in Figure 13.

Table 9:Development of absorbance at 25 and 30°C.

Absorbance values at 25°C				Absorbance values at 30°C							
Time (min)	20 ppm	40 ppm	60 ppm	Time (min)	20 ppm	40 ppm	60 ppm	Time (min)	20 ppm	40 ppm	60 ppm
0	0.58601	1.055588	1.390073	0	0.649226	1.067942	1.450631	102	0.597867	1.011056	1.493927
5.5	0.638586	1.173566	1.624859	6	0.663136	1.115726	1.599159	108	0.593978	1.00757	1.48992
10	0.644533	1.184439	1.676305	12	0.663476	1.108283	1.614834	114	0.590884	1.004052	1.485562
15	0.647445	1.184734	1.693845	18	0.659454	1.097604	1.606712	120	0.587488	1.00139	1.480414
20	0.648101	1.183771	1.694806	24	0.655549	1.089289	1.595513	126	0.584065	0.998956	1.47634
25	0.648147	1.179798	1.689884	30	0.650745	1.08012	1.583081	132	0.581146	0.99639	1.472032
30	0.648395	1.175163	1.684525	36	0.645538	1.07183	1.57253	138	0.57767	0.994919	1.468372
35	0.647106	1.17033	1.678731	42	0.640747	1.064211	1.56327	144	0.575033	0.99326	1.465157
45	0.645911	1.162348	1.666755	48	0.635995	1.056877	1.553264	150	0.571858	0.991781	1.4611
55	0.644023	1.15565	1.655187	54	0.631529	1.050925	1.543455	156	0.569312	0.991254	1.45785
65	0.642028	1.147818	1.646053	60	0.627125	1.043537	1.536105	162	0.566655	0.990776	1.45404
75	0.639041	1.140616	1.636106	66	0.622528	1.038319	1.52831	168	0.564254	0.991965	1.451657
105	0.632335	1.121978	1.613687	72	0.618031	1.032416	1.522349	174	0.561483	0.993176	1.450241
135	0.625359	1.106718	1.596881	78	0.613567	1.027195	1.516316	180	0.558776	0.998599	1.445734
165	0.618162	1.094515	1.582703	84	0.609442	1.022265	1.509585	186	0.555972	1.02415	1.444178
195	0.612099	1.083702	1.571864	90	0.605029	1.018857	1.504248	192	0.553865	1.023016	1.442103
				96	0.601531	1.014693	1.49932	198	0.551197	1.019739	1.439526

Note: This is the raw data for the information presented in Figure 14 (Top).

Table 10: Maximum absorbance values at 25 and 30˚C

Temperature	Sulfite concentration (PPM)					
	10	20	40	60	80	100
Maximum absorbance at 25°C	0.377877	0.648395	1.184734	1.694806	2.106418	2.447968
Maximum absorbance at 30°C	0.395318	0.663476	1.115726	1.614834	2.005241	2.275992

Note: this is the raw data for the information presented in Figure 14 (Bottom)

Table 11: Absorbance values for two White wines at set time points at different temperatures.

Wine	temp (°C)	Time (minutes)								
		0	6	12	18	24	30	36	42	48
Absorbance values of Wine 1	20	0.625557	0.818205	0.855569	0.874685	0.888195	0.900632	0.910935	0.919541	0.927812
	25	0.774028	0.919524	0.946001	0.96248	0.977232	0.991234	1.002884	1.012453	1.021376
	30	0.917331	1.061004	1.093235	1.113373	1.12666	1.140147	1.148585	1.156291	1.162787
	40	1.08362	1.245761	1.285207	1.30203	1.310677	1.315418	1.318839	1.320278	1.322069
Absorbance values of Wine 2	20	0.535973	0.677783	0.710749	0.729392	0.745856	0.760472	0.774581	0.786955	0.799645
	25	0.627607	0.747994	0.781733	0.805326	0.828633	0.847673	0.866116	0.883102	0.898886
	30	0.737069	0.868545	0.909079	0.937475	0.959708	0.981952	0.999385	1.013932	1.027782
	40	0.956405	1.110637	1.175171	1.212285	1.237282	1.254937	1.266247	1.277369	1.285126

Note: this is the raw data for the information presented in Figure 15

Wine 1: Wolf Blass – Red Label.
Semillon Sauvignon Blanc
2010, 13% alcohol

Wine 2: Clean Skins
Classic Dry White
2010, 13.4% alcohol

Table 12: Sulfite concentration at 48 minute time point

	Wine 1				Wine 2			
Temp (°C)	20	25	30	40	20	25	30	40
Sulfite Conc.	31.07347	35.08911	41.15823	47.99437	25.57274	29.83202	35.36405	46.40886

Note: this is the raw data for the information presented in Figure 16. Concentrations were determined using the calibration curve constructed in Figure 14 at 25°C. (Y= 0.0233X + 0.2038)

Table 13: Average absorbance values at the maximum and at 532 nm for three white wines at set time points

	Absorbance values					
Time (Sec)	Maximum absorbance			Absorbance at 532 nm		
	Wine 3	Wine 4	Wine 5	Wine 3	Wine 4	Wine 5
0	0.12883	0.146474	0.171779	0.108443	0.120939	0.143905
30	0.436568	0.454332	0.600483	0.327291	0.340243	0.449474
60	0.701994	0.71858	0.969382	0.51034	0.522973	0.704547
90	0.89803	0.915078	1.240365	0.644873	0.657975	0.891113
120	1.03969	1.057019	1.440819	0.742601	0.755701	1.030533
150	1.14169	1.160371	1.586331	0.813356	0.828389	1.133764
180	1.216533	1.235854	1.695542	0.865718	0.882194	1.211386
210	1.270839	1.291618	1.778726	0.904777	0.92293	1.270745
240	1.311041	1.332364	1.840429	0.934183	0.952823	1.3164
270	1.341118	1.363974	1.887982	0.955964	0.976132	1.351531
300	1.362609	1.386117	1.923327	0.973495	0.994021	1.378971
330	1.379789	1.403804	1.952193	0.986632	1.008212	1.400729
360	1.392261	1.416748	1.975001	0.997314	1.019716	1.418064
390	1.402061	1.426784	1.993063	1.005208	1.028375	1.43165
420	1.409834	1.435529	2.005049	1.012193	1.03542	1.44258
450	1.414523	1.441672	2.017027	1.017645	1.041533	1.451515
480	1.419297	1.446248	2.025673	1.022328	1.046329	1.459364
510	1.422682	1.451132	2.031916	1.025512	1.05177	1.465848
540	1.425529	1.454384	2.036459	1.028645	1.054854	1.470922
570	1.427948	1.456842	2.042254	1.031527	1.058654	1.475318

Note: This is the raw data that is presented in Figure 18.

Wine 3:Deakin estate
Sauvignon Blanc
2010, 11% alcohol

Wine 4: Bailey &Bailey, Legs eleven
Sauvignon Blanc
2010, 11% alcohol

Wine 5: Jacobs Creek
Sauvignon Blanc
2011, 11% alcohol

Table 14: Concentration of Sulfites in 3 white wines determined using the industry standard, the aspiration method

	Initial titre (mL)	Final titre (mL)	Difference (mL)	Sulfite Concentration (PPM)	Average Concentration ± Std deviation
Wine 3	12.6	13.9	1.3	20.8	20.26 ± 0.92376
	13.9	15.1	1.2	19.2	
	15.1	16.4	1.3	20.8	
Wine 4	1.6	3.0	1.4	22.4	21.33 ± 0.92376
	3.0	4.3	1.3	20.8	
	4.3	5.6	1.3	20.8	
Wine 5	6.2	8.2	2.0	32.0	30.93 ±1.8475
	8.2	10.0	1.8	28.8	
	10.0	12.0	2.0	32.0	

Note: This is the raw data which is presented in Figure 19 (horizontal lines).

Table 15: Concentration of Sulfites in 3 white wines determined using the absorbance values in table 13 and the calibration curves in Figure 17.

Sulfite concentration						
Time (sec)	At Maximum absorbance			At 532 nm		
	Wine 3	Wine 4	Wine 5	Wine 3	Wine 4	Wine 5
0	-0.09336	0.231565	2.916933	0.351763	0.676333	1.27286
30	5.573995	5.901145	10.81203	6.036128	6.372558	9.209711
60	10.46213	10.76759	17.60575	10.79064	11.11878	15.83498
90	14.07237	14.38633	22.59623	14.285	14.62532	20.68085
120	16.68121	17.00034	26.28783	16.82341	17.16366	24.30216
150	18.55966	18.9037	28.96761	18.6612	19.05165	26.98347
180	19.93799	20.29381	30.97887	20.02124	20.4492	28.99963
210	20.9381	21.32077	32.51078	21.03577	21.50727	30.54144
240	21.67846	22.07116	33.64713	21.79955	22.28373	31.72728
270	22.23238	22.65329	34.52287	22.3653	22.88914	32.63977
300	22.62815	23.06108	35.1738	22.82066	23.3538	33.35248
330	22.94454	23.38681	35.7054	23.16187	23.7224	33.91762
360	23.17424	23.62519	36.12543	23.43933	24.0212	34.36789
390	23.35472	23.81002	36.45806	23.64435	24.24611	34.72077
420	23.49786	23.97106	36.6788	23.82579	24.42909	35.00468
450	23.58422	24.0842	36.89939	23.96739	24.58788	35.23676
480	23.67214	24.16848	37.05861	24.08904	24.71245	35.44061
510	23.73447	24.25841	37.1736	24.17173	24.85377	35.60905
540	23.7869	24.3183	37.25725	24.25311	24.93388	35.74083
570	23.83145	24.36357	37.36398	24.32798	25.03256	35.85502

Note: This is the raw data that is presented in Figure 19

Table 16: Raw data collected to determine the calibration curve from 1-100ppmsulfites in solution using 7.8x10^{-4} mol/L PRA working solution (Fibre 1).

Sulfite concentration (ppm)	power (µW)				absorbance	length filled	absorbance per cm
	empty fibre		filled fibre				
	mean	st dev	mean	st dev			
10	651	5	231	3	0.45	18.80	0.02393
20	700	24	362	3	0.29	18.15	0.01578
50	592	24	216	5	0.44	17.97	0.02437
100	698	16	93	1	0.88	18.90	0.04632
30	614	27	235	10	0.42	18.90	0.02207
1	705	11	171	37	0.62	18.70	0.03290
10	658	18	41	4	1.21	18.50	0.06516
40	575	11	108	7	0.73	18.80	0.03863
60	599	6	154	2	0.59	18.90	0.03121
70	648	19	156	3	0.62	18.90	0.03272
80	630	7	130	1	0.69	18.90	0.03626
90	610	13	76	2	0.90	16.80	0.05384
90	653	6	120	2	0.74	18.75	0.03924
10	646	31	431	13	0.18	18.90	0.00930
1	689	30	436	16	0.20	18.90	0.01051
40	691	33	172	2	0.60	19.00	0.03179
40	655	9	160	6	0.61	18.80	0.03256

Note: This is the raw data that is presented in Figure 20. Data not included in the calibration curve is highlighted in red.

Table 17 Raw data collected to determine the calibration curve from 1-40ppm using 6.24x10^{-4} mol/L PRA working solution (Fibre 2).

concentration (ppm)	power (µW)				absorbance	length filled	absorbance per cm
	empty fibre		filled fibre				
	mean	st dev	mean	st dev			
30	49.4	2.5	4.1	0.3	1.08	13.50	0.08007
30	50.2	3	3.4	0.1	1.17	13.62	0.08587
10	51.3	2	7.45	0.4	0.84	13.83	0.06058
10	49.7	3	11.5	0.5	0.64	13.58	0.04680
10	50.4	2	8.46	0.3	0.78	13.75	0.05637
20	46.9	2	5.78	0.4	0.91	13.63	0.06669
20	48.6	3	6.15	0.4	0.90	13.67	0.06569
20	50.8	3	7.95	0.4	0.81	13.77	0.05851
5	49.8	2	13	0.5	0.58	13.75	0.04242
5	48.4	3	13.5	0.5	0.55	13.48	0.04113
5	51.1	3	14.1	0.7	0.56	13.65	0.04097
1	49.1	2	16	0.7	0.49	13.77	0.03537
1	49	2	20	0.7	0.39	13.70	0.02841
40	50.4	1.4	3.3	0.1	1.18	13.70	0.08642
40	48.1	0.8	3.58	0.2	1.13	13.53	0.08337
0	50	1.5	6.68	0.3	0.87	15.63	0.05592
0	48.9	3	16.6	0.5	0.47	13.70	0.03425

Note: This is the raw data that is presented in Figure 21.